R. & M. No. 3720

R. & M. No. 3720

MINISTRY OF DEFENCE (PROCUREMENT EXECUTIVE)

AERONAUTICAL RESEARCH COUNCIL

REPORTS AND MEMORANDA

An Experimental Investigation of the Subsonic Longitudinal Characteristics of Five Slender-Wing Models with Gothic Planforms

By D. L. I. KIRKPATRICK AND D. A. KIRBY

Aerodynamics Dept., R. A. E. Farnborough

LONDON: HER MAJESTY'S STATIONERY OFFICE

1973

PRICE £1·75 NET

An Experimental Investigation of the Subsonic Longitudinal Characteristics of Five Slender-Wing Models with Gothic Planforms

By D. L. I. KIRKPATRICK AND D. A. KIRBY

Aerodynamics Department, R. A. E., Farnborough

Reports and Memoranda No. 3720*
July, 1971

Summary

The lift, drag and pitching moment on five symmetrical slender-wing models with sharp edges and aspect ratios of 1·28 and 1·46 have been measured at low subsonic speed. Four of the models had a gothic planform and one a mild gothic planform. Variations in thickness distributions were covered by the range of models and the tests included a modification of one of the models to reduce the lift-dependent drag.

These tests extended earlier work on slender wings to higher aspect ratios and the results have been analysed to show how the lift, drag and longitudinal stability of wings in this higher range of aspect ratio are affected by planform shape and by the chordwise and spanwise distribution of wing thickness.

* Replaces R.A.E. Technical Report No. 71137—A.R.C. 33 473

LIST OF CONTENTS

1. Introduction

In the last few years, the effects of changes in various geometric parameters on the subsonic longitudinal characteristics of the slender wing have been investigated in the 4 ft × 3 ft wind tunnel at Farnborough by a series of linked experiments in which the systematic variation of one parameter at a time was undertaken. By using thin wings, it was possible to distinguish the influence of various types of planform on the lift, drag and pitching moment of the slender wing with sharp edges and to derive simple curves which can be used to estimate the subsonic longitudinal stability characteristics of thin slender wings[1,2,3]. The major effects of increasing wing thickness on these subsonic characteristics were demonstrated by tests on a delta wing of 70 degrees sweepback[4].

These experimental results, and the results of some tests made several years ago by Peckham[5] in the 13 ft × 9 ft wind tunnel at Bedford, have been used as a basis for two figures which summarize the more important features of the subsonic performance and longitudinal stability of symmetrical slender wings[6]. In these figures, reproduced as Figs. 1 and 2 of this Report, the lift-dependent drag parameter K/A and the angle of incidence α appropriate to a lift coefficient of 0·5, are taken as indicative of the performance in the take-off and landing phases of flight. Difficulty in balancing an aircraft is represented in the figures by the magnitude of the distance h_n between the aerodynamic centre and the centre of area of the wing planform; although a gross simplification of a major problem, the use of this parameter is convenient as a useful guide when assessing the suitability of various wing shapes. The difference Δh_n between the values of h_n at two different lift coefficients gives an indication of the curvature of the pitching moment characteristic and hence whether an aircraft based on a particular slender wing might present awkward stability and trimming problems. An ideal aircraft wing would have, within its operating range of lift coefficient, low lift-dependent drag to give good performance, small angles of incidence at take-off and landing to avoid cabin floor angle and ground clearance problems, and values of h_n and Δh_n small enough to facilitate balancing and control.

In Figs. 1 and 2, the shape of the symbols shows whether the wing considered had a gothic, delta or ogee-type of planform and data specifying the planform and thickness of each wing are tabulated in Table 1. Fig. 1, based on $C_L = 0{\cdot}5$, shows that improved performance (lower K/A) can be achieved by increasing the wing aspect ratio A or the planform shape parameter p, though in both cases the value of h_n/c increases. On the other hand increasing the wing thickness reduces both K/A and h_n/c; as explained in Ref. 4, the lift-dependent drag factor K decreases because the suction forces induced by the leading-edge vortices have an increasingly large forward component in the plane of the wing, and the distance h_n/c decreases because the point of action of the vortex-induced component of the normal force moves rearward as the wing thickness increases. Values of K/A and h_n/c are shown for lift coefficients of 0·2 and 0·5 in Fig. 2 and this demonstrates the advantages of the gothic type of planform in keeping Δh_n small.

From this analysis it was inferred that better performance might be achieved by using slender wings with aspect ratios nearer 1·5 and higher planform parameters than those previously tested. It was expected that such new wings, if their thickness distributions were similar to those of the earlier wings, would have relatively large values of h_n. However it was hoped that these values could be appreciably reduced by altering the form of the wing thickness distribution since this had been shown[7,8] to affect the leading-edge vortex development and hence the chordwise distribution of aerodynamic loading.

This Report presents the results of tests on a group of five symmetrical gothic and mild gothic models with aspect ratios of either 1·277 or 1·456. Their thickness distributions spanwise were such that the ratio of frontal area to plan area was 0·08, a value used previously on a delta wing of aspect ratio 1·456[4] and one which might be appropriate for an allwing slender aeroplane carrying about 300 passengers[9]. The chordwise thickness distributions of three of the wings were the same as the delta wing but for the other two the position of the maximum thickness was moved forward. In addition to these main tests another form of thickness distribution was tried in an experiment where one of the wings was modified in the manner suggested by Lee[10] to give more forward-facing surface under the leading-edge vortices and hence reduce drag.

The wing shapes are described in detail in Section 2, the experimental procedure in Section 3 and the calculation of results in Section 4. In Section 5 the experimental results are analysed and compared with

previous results to show how the use of larger aspect ratios and modifications to thickness distributions affected the subsonic lift, drag and longitudinal stability characteristics.

2. Details of Wings Tested

The first three models tested comprised one mild gothic and two gothic wings (see Fig. 3). The mild gothic and one of the gothic wings had the same aspect ratio ($A = 1{\cdot}456$) while the remaining gothic wing had a different aspect ratio ($A = 1{\cdot}277$) but the same slenderness ratio ($s(c)/c = 0{\cdot}424$) as the mild gothic wing. These three wings each had a thickness/chord ratio of 0·08, and a thickness distribution such that all the chordwise sections were of the same form. This distribution was specified by the equation

$$\frac{t}{c - x_0} = 0{\cdot}4156\frac{x - x_0}{c - x_0}\left(1 - \frac{x - x_0}{c - x_0}\right)\left(1 - \frac{x - x_0}{2(c - x_0)}\right)$$

where c is the wing chord, t is the wing thickness at a point (x, y) and (x_0, y) is a point on the leading edge. This particular thickness distribution was chosen so that the results of the tests on these three wings could be compared with those on the delta wing ($A = 1{\cdot}456$, $t/c = 0{\cdot}08$) of the same thickness distribution tested previously[4].

When this first set of three wings had been tested, one of them, the gothic model of aspect ratio $A = 1{\cdot}277$, was modified in an attempt to reduce its drag by increasing the forward component of the suction force induced by the leading-edge vortices. The position at each chordwise station of the vortices above the wing at an arbitrary chosen incidence $\alpha = 14{\cdot}6$ deg ($\alpha/\cot\varphi(0) = 0{\cdot}3$, $C_L \simeq 0{\cdot}57$) was calculated using a semi-empirical theory[7], and the wing was altered to increase the value of $\partial z/\partial x$ on the parts of the upper surface where the vortices were expected to induce high suction forces. Material was cut from the model to make part of the upper surface perpendicular to a ray from a calculated vortex position and to reduce the outer part of the wing to half its previous thickness (*see* Fig. 4a); the corners in the resulting spanwise cross sections were rounded to avoid discontinuities in $\partial t/\partial y$ which might lead to flow separations. During this modification equal amounts of material were cut from the upper and lower surfaces to ensure that the wing would remain symmetrical and its characteristics would be free from camber effects*. It should be emphasized that the form of this modification was guided largely by intuition, and the results of the exploratory tests on the modified wing do not represent the optimum that could be achieved by altering the spanwise distribution of wing thickness in order to reduce lift-dependent drag.

The next wing tested had a gothic planform with an aspect ratio $A = 1{\cdot}277$ and its thickness/chord ratio was equal to 0·08. The thickness distribution was such that all chordwise sections were of the same form and was specified by the equation

$$\frac{t}{c - x_0} = 0{\cdot}540\frac{x - x_0}{c - x_0}\left(1 - \frac{x - x_0}{c - x_0}\right)^2.$$

With this thickness distribution the position of maximum thickness was at $x_t/c = 0{\cdot}333$ instead of at $x_t/c = 0{\cdot}423$ for the first set of wings (*see* Table 2). It was expected, in view of the results of earlier analysis[8] of the aerodynamic loading distribution on slender wings, that this forward movement of the maximum thickness would decrease the load on the front part of the wing and hence reduce the value of h_n/c.

The thickness distribution of the wings described above, *viz.* all chordwise sections of the same form, is simple but has two significant disadvantages. For wings with streamwise tips the condition that the thickness/chord ratio is constant across the span yields near the trailing edge spanwise cross-sections with large edge angles, and experiments in conical flow have shown[7] that cross-sections with large edge angles induce much weaker leading-edge vortices than cross-sections with sharper edges. The other disadvantage is that in a plan view the leading-edge vortices cross the maximum thickness line so that the drag reduction due to high suction forces on the wing where $\partial z/\partial x$ is positive near the leading edge is

* Note: This modification reduced the value of Φ/S to 0·075 compared with 0·08 for the other wings.

partially counterbalanced by a drag increase due to high suction forces where $\partial z/\partial x$ is negative near the trailing edge. Accordingly the drag induced on a wing with constant thickness/chord ratio is greater than that on a wing with greater thickness near the centre line and less near the tips. To illustrate this effect, another gothic wing was made with a thickness/chord ratio which decreased towards the tips according to the equation

$$\frac{t}{c - x_0} = \left(\frac{t}{c}\right)_0 \frac{c - x_0}{c},$$

where $(t/c)_0$ is the thickness/chord ratio on the centre line. This gothic wing had an aspect ratio of 1·456 and its thickness distribution was specified by the equation

$$\frac{t}{c - x_0} = 1{\cdot}012 \frac{x - x_0}{c - x_0}\left(1 - \frac{x - x_0}{c - x_0}\right) \frac{c - x_0}{c}.$$

The value of $(t/c)_0$ was chosen to be 0·1067 so that the ratio of the frontal area to plan area of this wing (=0·08) was the same for this wing as for the other four. This thickness distribution has the point of maximum thickness at $x_t/c = 0{\cdot}25$ and is compared with other chordwise thickness distributions in Fig. 4b.

All the models were made of a resin-bonded glasscloth laminate sandwiched between two teak fairings; the use of glasscloth allowed the leading edges to be better defined and less fragile than if teak had been used throughout. Details of the geometry of each of the wings tested are presented in Table 2.

3. Experimental Procedure

The wings were hung successively from the standard wire rig of the 4 ft × 3 ft wind tunnel and on each wing measurements of the lift, drag and pitching moment were made over an angle of incidence range $-5 < \alpha < 26$ deg. The wind speed was 61 m/s (200 ft/s) giving a Reynolds number based on centre-line chord of between 1·5 and 2 million for the range of wings tested. When the force measurements had been completed, surface flow patterns were produced by mounting each wing on a sting support rig, painting the wing with a suspension of lampblack in paraffin, increasing the wind speed swiftly to the appropriate value and keeping it constant while the suspension dried.

In general the flow round a thin slender wing is virtually independent of scale effect provided that the wing's leading edges are sufficiently sharp to induce leading-edge separation at all non-zero incidences (*see* Section 4 of Ref. 1). But tests on thick slender wings have shown[4] that the laminar flow over such wings at low incidence may separate aft of the maximum thickness line inducing weak swept vortices and distorting the low-incidence end of the lift and pitching moment characteristics. During those tests it was found that such separations could be suppressed by fixing strips of carborundum on both surfaces near the leading edge and that, provided the strips of roughness were narrow, their presence did not affect the shape of the lift, drag or pitching moment characteristics at higher incidences.

In the present series of tests it was found that laminar flow separation occurred aft of the maximum thickness line on some of the wings at low incidence. In these cases, the separations were suppressed by roughness strips which were similar to those used in earlier tests[4] and were found to have no significant effect on the longitudinal characteristics at higher incidences (*see* tables).

Surface flow patterns on the gothic wing, $A = 1{\cdot}277$, $\Phi/S = 0{\cdot}075$, with material cut away near its leading edge, showed that at an incidence $\alpha \simeq 15$ deg with free transition the pattern over the rear two thirds of the wing was consistent with the desired flow (*see* Fig. 5a). However, over the front third the outflow beneath each vortex separated at the shoulder giving an unusually large secondary vortex and displacing the primary vortex inboard (*see* Fig. 5b). A strip of roughness 2·5 mm (0·1 in) wide was therefore placed just inboard of the shoulder over the front third of the wing and fresh surface flow patterns indicated that this strip prevented the shoulder separation (*see* Fig. 5c). Despite the change in the flow, the presence of the roughness strip had no appreciable effect on the longitudinal characteristics (*see* Tables).

4. Calculation of Results

The lift, drag and pitching moment coefficients were calculated by dividing the measured forces and moments by qS and qSc respectively, where q is the free stream dynamic pressure, S is the wing plan area and c the centre-line chord. These coefficients were then corrected for the effects of wind-tunnel blockage and constraint. Although the wings were nominally symmetrical, the very small lift forces and pitching moments measured at nominal zero incidence showed that some small asymmetries were present. Corrections for these distortions were made to the angle of incidence and the pitching moment coefficient to ensure that zero lift and pitching moment occurred at zero incidence, and the corrected coefficients are presented in Tables 3 to 8.

In studies of the influence of the various factors which govern the forces on a slender wing, it is more convenient from both theoretical and experimental standpoints to consider the flow relative to body rather than to wind axes. The measured lift and drag coefficients were therefore used to calculate the normal force coefficient

$$C_N = C_L \cos \alpha + C_D \sin \alpha,$$

and the axial force coefficient

$$C_A = -C_L \sin \alpha + C_D \cos \alpha,$$

and these coefficients are also included in Tables 3 to 8.

The lift, drag and pitching coefficients for the gothic and mild gothic wings in the present series, and for a delta wing tested previously[4], were plotted against incidence in Figs. 6–8. The symbols used to represent the various wings in these figures are retained throughout this Report and are summarised in Table 2.

5. Discussion and Analysis of Results

5.1. Lift

The lift characteristics plotted in Fig. 6 show that the lift on a slender wing of aspect ratio $A = 1{\cdot}456$ increases as its planform parameter p increases. This figure also shows that the lift of a slender wing can be increased by sharpening its leading edge or by moving forward the point of maximum thickness of the chordwise cross-section.

The lift characteristics of the gothic and mild gothic wings tested (and their pitching moment characteristics plotted in Fig. 8) 'jink' at a moderate angle of incidence. The extent of the jink, and the incidence at which it occurs, seem to depend on the aspect ratio and planform of the wing considered, as shown in the table below.

A	p	Jink incidence, deg
1·456	0·583	14–19
1·456	0·667	12–14
1·277	0·667	13–15

The jinks were attributed to the breakdown of the leading-edge vortices, because an earlier study[11] of vortex breakdown above wings of different aspect ratio and planform, had indicated that breakdown should occur above the present series of wings at incidences not far from the measured values tabulated above.

5.2. Normal Force

The analysis of the measured normal force on each wing follows the established principle[1,12] that the flow past a slender wing with sharp edges can be considered as the sum of two velocity fields, the linear and the nonlinear. The linear field is associated with the attached flow round the wing assumed to occur in slender-body theory[13] and yields a lifting force which is directly proportional to the angle of incidence. The non-linear field is associated with the leading-edge vortices which induce a force which is a non-linear function of incidence. Hence the normal force coefficient is written as

$$C_N = C_{N_l} + C_{N_{nl}} = \alpha\left(\frac{dC_N}{d\alpha}\right)_0 + C_{N_{nl}},$$

where C_{N_l} and $C_{N_{nl}}$ are the linear and non-linear components of the normal force coefficient C_N and $(dC_N/d\alpha)_0$ is the slope of the normal force characteristic at zero incidence.

In order to determine the value of $(dC_N/d\alpha)_0$ for each wing, the measured values of C_N/α were plotted against incidence in Fig. 9 and curves were drawn through each set of plotted points to intercept the C_N/α axis at $(C_N/\alpha)_0 = (dC_N/d\alpha)_0$. The values of $(C_N/\alpha)_0$ for each wing were then plotted in Fig. 10a which shows that the experimental values are considerably smaller than the value $(C_N/\alpha)_0 = \pi A/2$ predicted by slender-body theory[13]. Fig. 10b show the variation of the measured values of $(C_N/\alpha)_0$ with a parameter $A(1 + c_{0\cdot99}/c)$ devised by Kirby[1] to correlate the values of $(C_N/\alpha)_0$ for wings of different planform. This figure shows that the values of $(C_N/\alpha)_0$ for the wings where $x_t/c = 0{\cdot}423$ fall below the correlating curve because the present set of wings are thicker than those tested earlier. The values of $(C_N/\alpha)_0$ for the two wings where $x_t/c < 0{\cdot}423$ are significantly larger than the others, showing that the chordwise distribution of wing thickness has an appreciable effect on the linear component of the normal force which increases as the point of maximum thickness moves forward.

The experimental values of $(C_N/\alpha)_0$ were then used to obtain the non-linear component of the normal force, expressed as $\Delta(C_N/\alpha) = C_N/\alpha - (C_N/\alpha)_0$. Following the example of an earlier analysis[1] on low-aspect-ratio slender wings the values of $\Delta(C_N/\alpha)$ were divided by an empirical correlating parameter $A\eta$, where $\eta = s(x')/s(c)$ and $x' = c - s(c)$, and plotted against α/A in Fig. 11. This figure shows that the value of $\Delta(C_N/\alpha)/A\eta$ for a slender wing of aspect ratio $A = 1{\cdot}456$ generally decreases with increasing planform parameter and thus suggests that the correlating factor η is not completely valid for wings of comparatively high aspect ratio. The values of $\Delta(C_N/\alpha)$ for the wing with material cut away near its leading edges (*see* Fig. 4a) are somewhat higher than those for the unmodified wing, indicating that the sharper leading edge produces a stronger leading-edge vortex in accordance with the results of tests[7] in conical flow. The values of $\Delta(C_N/\alpha)$ for the wings having $x_t/c < 0{\cdot}423$ are appreciably smaller than the corresponding values on wings where $x_t/c = 0{\cdot}423$. Experimental investigations[7] have shown that the chordwise growth $\partial\Gamma/\partial x$ of the strength of a leading-edge vortex is approximately proportional to $\partial s/\partial x$, so that for a plane gothic wing more than half the strength of the leading-edge vortices comes from vorticity shed from the front third of the leading edge, and also to $(1 - n)$ where $n\pi$ is the leading-edge angle of the wings' spanwise cross-section. Consequently it is probable that forward movement of the point of maximum thickness, by increasing $n\pi$ near the apex, reduces the vorticity shed from that part of the wing which contributes most of the strength of the leading-edge vortex and hence to the non-linear component of the normal force.

5.3. Axial Force and Drag

The variation with incidence of the difference between the axial force coefficient C_A and the profile drag coefficient C_{D_0} on each of the wings tested was plotted in Fig. 12. To eliminate the effects of low values of drag in the laminar drag bucket near zero lift, the values of C_{D_0} were obtained by extrapolation of the drag values measured at moderate incidence. The values of the vortex-induced thrust $C_{D_0} - C_A$ at chosen values of incidence were then divided by the ratio of the forward-facing area Φ and the plan area S, and the variation of $(C_{D_0} - C_A)/(\Phi/S)$ with $C_{N_{nl}}$ for each wing was plotted in Fig. 13, together with the results for a delta wing tested previously[4].

The upper part of Fig. 13 shows that $(C_{D_0} - C_A)/(\Phi/S)$ increases as the slenderness ratio $s(c)/c$ increases and that the vortex-induced thrust on wings with a given thickness distribution may be approximated by the expression

$$C_{D_0} - C_A = \frac{\Phi}{S} \frac{s(c)}{c} f(C_{N_{nl}}),$$

where $f(C_{N_{nl}})$ is a function of the non-linear component of the normal force.

Fig. 13 shows that at low incidences and small values of $C_{N_{nl}}$ the vortex-induced thrust parameter $(C_{D_0} - C_A)/(\Phi/S)$ on the modified wing, with $\Phi/S = 0{\cdot}075$, was less than that on the unmodified wing, because at such incidences the modified wing had less forward-facing area under the vortices, but was greater than that on the unmodified wing at higher incidences; Fig. 12 shows that the largest increment occurs at about $\alpha = 19$ deg. This incidence is rather larger than the design incidence, i.e. the incidence at which the maximum improvement in performance was expected (*see* Section 2), probably because the vortex development was predicted for a wing of zero thickness and the finite thickness of the wing tested delayed the inboard movement of the leading-edge vortex with incidence[6]. It must be remembered that at $\alpha = 19$ deg the increment $(\Delta(C_{D_0} - C_A) \simeq 0{\cdot}005)$ in the vortex-induced thrust on the modified wing was achieved despite the occurrence of undesirable flow separations on the forward part of the wing (*see* Section 3 and Fig. 5b) which includes a large proportion of the forward-facing area. It is not unreasonable to expect that smoothing the spanwise profile to suppress these separations could considerably increase the thrust increment and hence improve performance, e.g. at $C_L = 0{\cdot}5$ an increment of 0·01 in $C_{D_0} - C_A$ would reduce the lift-dependent factor K of this wing by approximately 0·15.

Fig. 13 shows that at a given value of $C_{N_{nl}}$ the thrust parameter $(C_{D_0} - C_A)/(\Phi/S)$ increases as the point of maximum thickness moves forward. This increase of the thrust parameter with decreasing x_t occurs because moving the maximum thickness forward increases the slope $\partial z/\partial x$ of the upper surface near the apex which sustains high vortex-induced suction forces and thus increases the forward component of these forces. Moving the maximum thickness forward also reduces the vortex strength and hence $C_{N_{nl}}$ (*see* Fig. 11), but the concurrent effect on the upper-surface slope is powerful enough to yield significant increases in the vortex-induced thrust $C_{D_0} - C_A$ at constant incidence (*see* Fig. 12). The results for the two wings of aspect ratio $A = 1{\cdot}456$ suggest that a further increase of $C_{D_0} - C_A$ has been achieved by reducing the wing thickness near the tips while increasing it at the centre-line (as discussed in Section 2). The table below shows that these changes in the chordwise and spanwise distribution of wing thickness have a significant effect on the vortex-induced thrust, and it is reasonable to expect that further refinement of the thickness distribution would yield increases of $C_{D_0} - C_A$ even greater than the 38 per cent measured in these tests.

A	x_t/c	α, deg	$C_{D_0} - C_A$	% increase
1·277	0·423	15	0·0275	–
1·277	0·333		0·0325	18
1·456	0·423		0·0305	–
1·456	0·250		0·0420	38

The values of the lift-dependent drag factor $K = \pi A(C_D - C_{D_0})/C_L^2$ were calculated and plotted against the lift coefficient in Fig. 14 which shows how the lift-dependent drag of a slender wing is affected by its planform and thickness distribution. It has been demonstrated[4] that the factor K may be approximated by the expression

$$K = \frac{\pi A}{C_L}\left(\tan\alpha - \frac{C_{D_0} - C_A}{C_N}\right).$$

For a wing of zero thickness, K is determined entirely by the drag force ($=C_L \tan \alpha$) arising from the resolution of the normal force, but for wings of finite thickness the suction induced by the leading-edge vortices on forward-facing surfaces yields a thrust component $C_{D_0} - C_A$. Fig. 15 presents a breakdown of the lift-dependent drag on a thick slender wing and compares K with $\pi A \tan \alpha / C_L$ and with $\pi A \tan \alpha / C_{L_i}$, where C_L is the measured lift coefficient at wing incidence α and $C_{L_i} = (C_N/\alpha)_0 \alpha \cos \alpha$ is the linear component of the lift coefficient. This figure shows that both the non-linear lift induced by the leading-edge vortices and the thrust due to vortex-induced suction on forward-facing surfaces have important effects on the lift-dependent drag of a slender wing.

5.4. Pitching Moment

Fig. 8 shows the variation with incidence of the pitching moment coefficient on each of the wings tested. This figure shows that as the incidence increases from zero the pitching moment of the gothic wings first increases and then decreases over most of the incidence range but this decrease is interrupted by the effects of vortex breakdown.

The distance x_n from the apex to the aerodynamic centre was calculated for each wing using the equation

$$x_n = x_m - \frac{\partial C_m}{\partial C_N} c,$$

where x_m is the distance from the apex to the moment centre, and the distance h_n from the centre of area to the aerodynamic centre from the equation

$$h_n = x_{ca} - x_n.$$

The values of x_n were plotted in Fig. 16 which shows that, after an initial abrupt rearward movement as C_L increases from zero, the aerodynamic centre of each of the gothic wings moves slowly rearward as C_L increases, except in regions where vortex breakdown effects are apparent. In such regions it is not possible to define accurately the slope of the pitching moment characteristic and the curves in Fig. 16 are dotted to indicate uncertainty. Further detailed investigations of the occurrence and effect of vortex breakdown would be necessary before sustained flight in these regions could be contemplated. Despite the regions of uncertainty, Fig. 16 shows that the position of the aerodynamic centre is appreciably affected by changing the chordwise thickness distribution and moves rearward as the point of maximum thickness moves forward.

Changing the chordwise thickness distribution of a slender wing does not alter the centre of area but does alter the centre of volume. For allwing layouts, the centre of volume may be considered to be more representative of the centre of gravity position than the centre of area, and the results of these tests show that, since the aerodynamic centre is moving rearward and the centre of volume forward with forward movement of maximum thickness, the chordwise distribution of wing thickness has an important effect on the longitudinal stability. The table below compares mean values of $(x_{ca} - x_n)/c$ and $(x_{cv} - x_n)/c$ for angles of incidence between $C_L = 0{\cdot}2$ and the occurrence of vortex breakdown.

A	p	x_t/c	x_{ca}/c	x_{cv}/c	x_n/c	$(x_{ca} - x_n)/c$	$(x_{cv} - x_n)/c$
1·277	0·667	0·423	0·625	0·573	0·488	0·137	0·085
1·277		0·333		0·520	0·498	0·127	0·022
1·456		0·423		0·573	0·485	0·140	0·088
1·456		0·250		0·444	0·495	0·130	−0·051

This table suggests that it might be possible to balance an allwing slender aeroplane with a gothic planform by suitable positioning of the point of maximum thickness and hence of the payload.

6. Concluding Remarks

The values of K/A and h_n/c at $C_L = 0{\cdot}5$ and $C_L = 0{\cdot}2$ for each of the wing shapes tested were plotted in Fig. 17 together with the results of earlier tests. It must be remembered that, at $C_L = 0{\cdot}5$, the results for some of the wings tested were affected by vortex breakdown. Fig. 17 shows that, at $C_L = 0{\cdot}5$, the present set of wings have lower values of incidence and K/A than wings tested previously but this improvement in performance has been attained at the cost of increasing h_n/c. Comparison of the results for the gothic wings with different chordwise thickness distributions shows that appreciable benefits, *viz.* lower incidence, lower K/A and lower h_n/c can be achieved by changes in thickness distribution.

The operational use of gothic wings having comparatively large planform parameters and aspect ratios, i.e. wings similar to those tested, may well be precluded by the onset of vortex breakdown and the associated problems of lateral instability and structural fatigue. But the results of these tests suggest that improved thickness distributions can be designed for all planforms to yield appreciably larger values of vortex-induced thrust, and consequently lower values of lift-dependent drag, than those measured hitherto. The simple changes in thickness distribution studied in this Report produced lift-dependent drag reductions of up to 9 per cent at $C_L = 0{\cdot}5$, and it is probable that more refined distributions would reduce the lift-dependent drag by as much again. Further substantial improvements in performance can be attained by cambering slender wings and the effectiveness of some camber designs is currently being investigated[14].

LIST OF SYMBOLS

A	aspect ratio
b	span
c	centre-line chord
$c_{0\cdot99}$	wing chord at $y = 0{\cdot}99b/2$
C_A	axial force coefficient
C_D	drag coefficient
C_{D_0}	drag coefficient at zero lift
C_L	lift coefficient
C_m	pitching moment coefficient
C_N	normal force coefficient
C_{N_l}	linear component of C_N
$C_{N_{nl}}$	non-linear component of C_N
h_n	$x_{ca} - x_n$
K	lift-dependent drag factor
$n\pi$	leading-edge angle of the wing's cross-section
p	planform parameter S/bc
$s(x)$	semispan at chordwise station x
S	wing area
t	wing thickness
x, y, z	orthogonal system of axes, x measured in chordal plane downstream from the apex, y spanwise and z normal to the wing
x_{ca}	distance from apex to the centre of area
x_{cv}	distance from apex to the centre of volume
x_m	distance from apex to the pitching moment centre
x_n	distance from apex to the aerodynamic centre
x_0	distance from apex to the leading edge
x_t	distance from apex to the point of maximum thickness
α	angle of incidence
Γ	circulation round a leading-edge vortex
η	$s(x)/s(c)$ where $x = c - s(c)$
Φ	wing frontal area
φ	leading-edge sweepback angle
$\varphi(x)$	leading-edge sweepback angle at station x

REFERENCES

No.	Author(s)	Title, etc.
1	D. A. Kirby	An experimental investigation of the effect of planform shape on the subsonic longitudinal stability characteristics of slender wings. A.R.C. R. & M. 3568 (1967).
2	A. G. Hepworth	The longitudinal stability characteristics of an ogee wing of slenderness ratio 0·35. A.R.C. C.P. 1227 (1971).
3	D. L. I. Kirkpatrick and A. G. Hepworth	Experimental investigation of the effect of trailing-edge sweepback on the subsonic longitudinal characteristics of slender wings. A.R.C. C.P. 1130 (1970).
4	D. A. Kirby and D. L. I. Kirkpatrick	An experimental investigation of the effect of thickness on the subsonic longitudinal stability characteristics of delta wings of 70 deg sweepback. A.R.C. R. & M. 3673 (1969).
5	D. H. Peckham	Low-speed wind-tunnel tests on a series of uncambered slender pointed wings with sharp edges. A.R.C. R. & M. 3186 (1958).
6	D. A. Kirby and D. L. I. Kirkpatrick	Selections from Aerodynamic Research at R.A.E.—1969. R.A.E. Technical Report 70059 A.R.C. 32190 (1970).
7	D. L. I. Kirkpatrick	A study of the leading-edge vortices above slender wings. University of Southampton, Ph.D. Thesis (1970).
8	D. L. I. Kirkpatrick	Analysis of the static pressure distribution on a delta wing in subsonic flow. A.R.C. R. & M. 3619 (1968).
9	D. Küchemann and J. Weber	An analysis of some performance aspects of various types of aircraft designed to fly over different ranges at different speeds. *Progress in Aero Sciences* Vol. 9, pp 329–456, Pergamon Press (1968).
10	G. H. Lee	Reduction of lift-dependent drag with separated flow. A.R.C. C.P. 593 (1959).
11	W. H. Wentz and D. L. Kolman	Wind-tunnel investigation of vortex breakdown on slender sharp-edged wings. University of Kansas Report FRL 68-013 (1968).
12	A. Spence and D. Lean ..	Some low-speed problems of high-speed aircraft. *Journal of the Royal Aero. Soc.*, Vol. 66, No. 616 (1962).

13 R. T. Jones .. .. .. Properties of low aspect ratio pointed wings at speeds below and above the speed of sound.
N.A.C.A. T.N. 1032 (A.R.C. 9483) (1946).

14 P. J. Butterworth .. .. Low-speed wind-tunnel tests on a family of cambered wings of mild gothic planform of aspect ratio 1·4.
A.R.C. C.P. 1163 (1970).

TABLE 1

Subsonic Longitudinal Characteristics of Slender Wings

Ref.	Planform	A	$\frac{s(c)}{c}$	p	$\left(\frac{t}{c}\right)_{max}$	$C_L = 0{\cdot}5$			$C_L = 0{\cdot}2$	
						K/A	h_n/c	α	K/A	h_n/c
↑	Delta	0·8	0·20	0·5	0·04	1·82	0·067	16·5	2·12	0·046
|		1·0	0·25			1·62	0·079	15·0	1·80	0·055
|		1·2	0·30			1·48	0·086	13·8	1·64	0·063
|		1·4	0·35			1·35	0·088	13·0	1·43	0·069
|		1·6	0·40			1·23	0·097	12·3	1·26	0·077
Kirby[1]										
|	Near Gothic	0·775	0·25	0·645	0·04	1·63	0·110	15·3	1·87	0·103
|		0·930	0·30			1·46	0·112	14·3	1·65	0·114
|	Ogee	0·841	0·20	0·476	0·04	1·72	0·050	15·8	1·94	0·029
|		1·051	0·25			1·52	0·063	14·3	1·62	0·036
|		1·262	0·30			1·35	0·068	13·2	1·41	0·045
↓										
Hepworth[2]	Ogee	1·462	0·347	0·476	0·04	1·26	0·074	12·2	1·32	0·049
↑	Delta	1·456	0·364	0·5	0·04	1·31	0·093	12·7	1·35	0·075
Kirby Kirkpatrick[4]					0·08	1·26	0·081	13·4	1·24	0·059
|					0·12	1·22	0·063	14·2	1·11	0·035
↓					0·16	1·19	0·044	15·0	1·10	0·023
↑	Delta	1·0	0·25	0·5	0·12	1·60	0·050	15·9	1·82	0·034
|	Delta				0·01	1·66	0·090	15·0	1·97	0·077
Peckham[5]	Gothic				0·12	1·40	0·105	14·1	1·75	0·118
↓	Gothic				0·01	1·46	0·132	13·7	1·71	0·135
Kirby[1]	Ogee	1·04	0·30	0·577	0·04	1·40	0·098	13·5	1·54	0·093

TABLE 2

Wing Geometry

Planform	A	$\frac{s(c)}{c}$	p	$\frac{x_{ca}}{c}$	$\left(\frac{t}{c}\right)_{max}$	$\frac{x_t}{c}$	$\frac{\Phi}{S}$	Symbol
Delta[4]	1·456	0·364	0·5	0·667	0·08	0·423	0·080	+
Mild gothic	1·456	0·424	0·583	0·653	0·08	0·423	0·080	×
Gothic	1·456	0·485	0·667	0·625	0·08	0·423	0·080	⊙
Gothic	1·277	0·424	0·667	0·625	0·08	0·423	0·080	⊡
Gothic	1·277	0·424	0·667	0·625	0·08	0·423	0·075	◪
Gothic	1·277	0·424	0·667	0·625	0·08	0·333	0·080	■
Gothic	1·456	0·485	0·667	0·625	0·107	0·250	0·080	●

Each wing had a span of 0·36 m (15 in).

TABLE 3

Mild Gothic Wing, A = 1·456, Transition Free

α, deg	C_L	C_D	C_N	C_A	C_m	C_N/α	K
−4·77	−0·1600	0·01665	−0·1608	0·0033	0·00061	1·9321	
−4·25	−0·1391	0·01427	−0·1397	0·0039	−0·00003	1·8835	
−3·73	−0·1165	0·01247	−0·1170	0·0048	−0·00064	1·7972	C_{D_0} =
−3·22	−0·1012	0·01119	−0·1016	0·0055	−0·00077	1·8094	0·0076
−2·71	−0·0865	0·01032	−0·0869	0·0062	−0·00091	1·8402	
−2·19	−0·0672	0·00916	−0·0675	0·0066	−0·00105	1·7676	
−1·68	−0·0542	0·00838	−0·0544	0·0068	−0·00092	1·8584	
−1·16	−0·0400	0·00680	−0·0401	0·0060	0·00014	1·9742	
−0·65	−0·0211	0·00645	−0·0211	0·0062	0·00003	1·8677	
−0·14	−0·0060	0·00633	−0·0060	0·0063	0·00002	2·5327	
0·38	0·0132	0·00625	0·0133	0·0062	0·00071	1·9928	
0·90	0·0313	0·00659	0·0314	0·0061	0·00045	2·0039	
1·41	0·0447	0·00671	0·0448	0·0056	0·00034	1·8224	
1·92	0·0596	0·00795	0·0599	0·0059	0·00110	1·7851	
2·43	0·0724	0·00924	0·0727	0·0062	0·00124	1·7131	
2·95	0·0921	0·01042	0·0925	0·0057	0·00118	1·7967	1·521
3·46	0·1075	0·01154	0·1080	0·0050	0·00101	1·7863	1·562
3·98	0·1290	0·01302	0·1296	0·0040	0·00059	1·8649	1·490
4·50	0·1460	0·01463	0·1467	0·0031	0·00022	1·8692	1·508
5·02	0·1689	0·01716	0·1697	0·0023	−0·00045	1·9383	1·534
5·53	0·1874	0·01752	0·1882	−0·0006	−0·00035	1·9489	1·293
6·57	0·2350	0·02646	0·2365	−0·0006	−0·00173	2·0614	1·562
7·61	0·2794	0·03457	0·2816	−0·0028	−0·00241	2·1191	1·580
8·65	0·3236	0·04385	0·3265	−0·0053	−0·00309	2·1624	1·583
9·69	0·3709	0·05563	0·3749	−0·0076	−0·00356	2·2164	1·597
10·74	0·4212	0·06968	0·4268	−0·0100	−0·00392	2·2777	1·601
11·83	0·4701	0·08503	0·4775	−0·0131	−0·00454	2·3130	1·603
12·82	0·5187	0·10231	0·5285	−0·0154	−0·00428	2·3616	1·610
13·87	0·5691	0·12176	0·5817	−0·0182	−0·00420	2·4036	1·613
14·97	0·6177	0·14284	0·6336	−0·0214	−0·00356	2·4271	1·822
15·95	0·6637	0·16533	0·6836	−0·0234	−0·00230	2·4561	1·638
16·98	0·7027	0·18670	0·7266	−0·0267	−0·00035	2·4515	1·659
18·02	0·7478	0·21389	0·7773	−0·0280	0·00011	2·4712	1·687
19·06	0·7848	0·23923	0·8199	−0·0301	0·00075	2·4655	1·720
20·09	0·8299	0·27036	0·8722	−0·0312	0·00024	2·4872	1·745
21.14	0·8804	0·30590	0·9314	−0·0322	−0·00026	2·5247	1·761
22·18	0·9234	0·33777	0·9826	−0·0358	−0·00068	2·5387	1·771
23·22	0·9754	0·37764	1·0453	−0·0376	−0·00145	2·5790	1·779
24·27	1·0278	0·42105	1·1100	−0·0386	−0·00182	2·6208	1·790
25·31	1·0741	0·45990	1·1676	−0·0434	−0·00220	2·6432	1·793
26·35	1·1187	0·50226	1·2254	−0·0465	−0·00241	2·6647	1·808

TABLE 3 (Contd)

Mild Gothic Wing, A = 1·456, Transition Fixed at Leading Edge

α, deg	C_L	C_D	C_N	C_A	C_m	C_N/α	K
−4·86	−0·1595	0·01826	−0·1605	0·0047	0·00027	1·8927	
−4·34	−0·1419	0·01651	−0·1428	0·0057	0·00008	1·8833	
−3·83	−0·1211	0·01467	−0·1218	0·0066	−0·00012	1·8241	C_{D_0} =
−3·31	−0·1062	0·01367	−0·1068	0·0075	−0·00012	1·8483	0·0097
−2·80	−0·0874	0·01259	−0·0879	0·0083	0·00002	1·8007	
−2·28	−0·0732	0·01209	−0·0736	0·0092	0·00007	1·8469	
−1·77	−0·0551	0·01146	−0·0554	0·0098	−0·00009	1·7969	
−1·26	−0·0406	0·01106	−0·0409	0·0102	0	1·8657	
−0·74	−0·0232	0·01082	−0·0233	0·0105	−0·00005	1·8036	
−0·23	−0·0087	0·01064	−0·0087	0·0106	0·00007	2·1929	
0·29	0·0091	0·01049	0·0091	0·0104	0·00030	1·8180	
0·80	0·0274	0·01078	0·0275	0·0104	0·00009	1·9610	
1·32	0·0450	0·01101	0·0452	0·0100	−0·00001	1·9633	
1·83	0·0597	0·01140	0·0600	0·0095	0·00003	1·8770	
2·35	0·0776	0·01204	0·0780	0·0089	−0·00018	1·9040	
2·86	0·0922	0·01262	0·0927	0·0080	0·00004	1·8574	1·571
3·38	0·1119	0·01385	0·1125	0·0072	−0·00028	1·9086	1·520
3·89	0·1272	0·01489	0·1279	0·0062	−0·00037	1·8841	1·467
4·41	0·1488	0·01695	0·1497	0·0055	−0·00083	1·9453	1·498
4·92	0·1662	0·01875	0·1672	0·0044	−0·00098	1·9450	1·499
5·45	0·1897	0·02159	0·1909	0·0035	−0·00168	2·0091	1·512
10·70	0·4231	0·07216	0·4291	−0·0076	−0·00441	2·2984	1·596
15·85	0·6571	0·16336	0·6767	−0·0224	−0·00284	2·4460	1·628
21·10	0·8832	0·30747	0·9347	−0·0311	−0·00174	2·5381	1·746
26·27	1·1287	0·50531	1·2357	−0·0464	−0·00060	2·6955	1·778

TABLE 4

Gothic Wing, A = 1·456, x_t/c = 0·423, Transition Free

α, deg	C_L	C_D	C_N	C_A	C_m	C_N/α	K
−4·63	−0·1579	0·01636	−0·1587	0·0036	−0·00194	1·9643	
−4·11	−0·1366	0·01433	−0·1372	0·0045	−0·00231	1·9129	
−3·59	−0·1174	0·01270	−0·1179	0·0053	−0·00245	1·8801	
−3·03	−0·0994	0·01138	−0·0998	0·0060	−0·00224	1·8587	
−2·56	−0·0807	0·01039	−0·0811	0·0068	−0·00218	1·8145	C_{D_0} =
−2·05	−0·0645	0·00902	−0·0648	0·0067	−0·00162	1·8130	0·0078
−1·54	−0·0510	0·00754	−0·0511	0·0062	−0·00081	1·9089	
−1·02	−0·0390	0·00724	−0·0391	0·0065	−0·00056	2·1868	
−0·51	−0·0214	0·00684	−0·0215	0·0067	−0·00030	2·4171	
0·01	−0·0038	0·00654	−0·0038	0·0065	0·00005	—	
0·53	0·0175	0·00654	0·0175	0·0064	0·00040	1·9097	
1·04	0·0354	0·00699	0·0355	0·0063	0·00053	1·9525	
1·56	0·0513	0·00775	0·0515	0·0064	0·00086	1·8955	
2·07	0·0661	0·00920	0·0664	0·0068	0·00198	1·8401	
2·58	0·0814	0·01018	0·0818	0·0065	0·00244	1·8142	
3·10	0·1004	0·01125	0·1009	0·0058	0·00256	1·8649	1·5677
3·62	0·1189	0·01253	0·1195	0·0050	0·00275	1·8937	1·5296
4·13	0·1387	0·01418	0·1394	0·0041	0·00259	1·9327	1·5162
4·65	0·1604	0·01633	0·1611	0·0033	0·00228	1·9849	1·5167
5·17	0·1828	0·01883	0·1838	0·0023	0·00197	2·0359	1·5098
5·74	0·2052	0·02154	0·2064	0·0009	0·00167	2·0593	1·4923
6·73	0·2440	0·02734	0·2455	−0·0014	0·00338	2·0915	1·5014
7·77	0·2891	0·03540	0·2913	−0·0040	0·00113	2·1491	1·5102
8·81	0·3358	0·04548	0·3388	−0·0065	0·00081	2·2044	1·5283
9·85	0·3836	0·05725	0·3878	−0·0092	0·00066	2·2558	1·5368
10·90	0·4347	0·07153	0·4404	−0·0119	0·00052	2·3161	1·5426
11·94	0·4840	0·08723	0·4915	−0·0148	0·00085	2·3591	1·5512
12·98	0·5343	0·10546	0·5443	−0·0173	0·00154	2·4021	1·5651
14·02	0·5757	0·12263	0·5883	−0·0205	0·00287	2·4041	1·5849
15·05	0·6279	0·14534	0·6441	−0·0226	0·00205	2·4511	1·5921
16·10	0·6701	0·16639	0·6900	−0·0260	0·00219	2·4549	1·6153
17·15	0·7242	0·19381	0·7491	−0·0284	0·00108	2·5025	1·6224
18·20	0·7783	0·22324	0·8091	−0·0310	−0·00095	2·5471	1·6269
19·25	0·8322	0·25521	0·8698	−0·0334	−0·00066	2·5891	1·6342
20·35	0·8880	0·29043	0·9335	−0·0365	−0·00172	2·6287	1·6396
21·34	0·9338	0·32233	0·9871	−0·0396	−0·00231	2·6504	1·6498
22·39	0·9909	0·35420	1·0550	−0·0408	−0·00382	2·6996	1·6602
23·43	1·0379	0·40192	1·1121	−0·0440	−0·00455	2·7192	1·6736
24·47	1·0818	0·44020	1·1670	−0·0475	−0·00569	2·7321	1·6901
25·52	1·1303	0·48606	1·2295	−0·0483	−0·00652	2·7608	1·7122
26·55	1·1700	0·52643	1·2819	−0·0521	−0·00740	2·7663	1·7329

TABLE 4 (Contd)

Gothic Wing, A = 1·456, x_t/c = 0·423, Transition Fixed at Leading Edge

α, deg	C_L	C_D	C_N	C_A	C_m	C_N/α	K
−4·65	−0·1578	0·01803	−0·1588	0·0052	−0·00220	1·9564	
−4·13	−0·1377	0·01614	−0·1385	0·0062	−0·00214	1·9202	
−3·62	−0·1205	0·01472	−0·1212	0·0071	−0·00183	1·9208	
−3·10	−0·1029	0·01362	−0·1035	0·0080	−0·00161	1·9130	
−2·58	−0·0843	0·01265	−0·0848	0·0088	−0·00141	1·8802	C_{D_0} =
−2·07	−0·0673	0·01193	−0·0676	0·0095	−0·00121	1·8727	0·0100
−1·56	−0·0547	0·01175	−0·0550	0·0103	−0·00105	2·0230	
−1·04	−0·0360	0·01123	−0·0362	0·0106	−0·00073	1·9909	
−0·53	−0·0195	0·01093	−0·0196	0·0108	−0·00029	2·1336	
−0·01	−0·0019	0·01083	−0·0019	0·0108	−0·00010	—	
0·50	0·0156	0·01088	0·0157	0·0108	0·00016	1·7868	
1·02	0·0324	0·01110	0·0326	0·0105	0·00083	1·8315	
1·53	0·0494	0·01134	0·0497	0·0100	0·00108	1·8557	
2·05	0·0671	0·01164	0·0675	0·0092	0·00124	1·8871	
2·56	0·0839	0·01236	0·0844	0·0086	0·00149	1·8863	
3·08	0·1017	0·01336	0·1022	0·0079	0·00182	1·9019	1·4854
3·59	0·1182	0·01450	0·1189	0·0071	0·00217	1·8956	1·4736
4·16	0·1366	0·01599	0·1374	0·0060	0·00242	1·8918	1·4687
4·63	0·1565	0·01771	0·1574	0·0050	0·00272	1·9486	1·4402
5·15	0·1780	0·02017	0·1791	0·0041	0·00234	1·9931	1·4684
5·67	0·2000	0·02270	0·2013	0·0028	0·00171	2·0352	1·4525
6·71	0·2454	0·02957	0·2472	0·0007	0·00159	2·1117	1·4872
7·75	0·2906	0·03782	0·2930	−0·0017	0·00128	2·1673	1·5069
8·79	0·3376	0·04802	0·3409	−0·0041	0·00108	2·2227	1·4531
9·83	0·3865	0·06001	0·3910	−0·0069	0·00087	2·2789	1·5315
10·93	0·4368	0·07359	0·4428	−0·0105	0·00080	2·3221	1·5247
11·92	0·4843	0·08826	0·4921	−0·0137	0·00103	2·3657	1·5264
12·96	0·5326	0·10596	0·5428	−0·0162	0·00244	2·3992	1·5479
14·00	0·5745	0·12278	0·5871	−0·0198	0·00298	2·4031	1·5606
15·04	0·6175	0·14233	0·6333	−0·0228	0·00272	2·4132	1·5876
16·08	0·6689	0·16627	0·6888	−0·0256	0·00227	2·4539	1·5978
17·13	0·7230	0·19376	0·7480	−0·0278	0·00234	2·5016	1·6082
18·18	0·7754	0·21736	0·8045	−0·0354	0·00102	2·5359	1·5773
19·23	0·8288	0·25088	0·8651	−0·0360	0·00016	2·5784	1·6043
20·28	0·8844	0·28645	0·9288	−0·0378	−0·00110	2·6249	1·6169
21·32	0·9298	0·31608	0·9811	−0·0436	−0·00153	2·6372	1·6197
22·37	0·9857	0·36248	1·0494	−0·0399	−0·00324	2·6884	1·6596
23·41	1·0371	0·40517	1·1127	−0·0403	−0·00423	2·7231	1·6807
24·44	1·0647	0·42846	1·1466	−0·0504	−0·00408	2·6884	1·6911
25·48	1·1064	0·46617	1·1993	−0·0550	−0·00472	2·6974	1·7053
26·51	1·1495	0·48820	1·2465	−0·0763	−0·00414	2·6937	1·6445

TABLE 5

Gothic Wing, A = 1·277, x_t/c = 0·423, Transition Free

α, deg	C_L	C_D	C_N	C_A	C_m	C_N/α	K
−4·73	−0·1463	0·01549	−0·1471	0·0034	−0·00147	1·7810	
−4·21	−0·1290	0·01369	−0·1296	0·0042	−0·00171	1·7623	C_{D_0} =
−3·69	−0·1074	0·01169	−0·1080	0·0047	−0·00209	1·6754	0·0076
−3·17	−0·0863	0·01024	−0·0867	0·0055	−0·00242	1·5671	
−2·65	−0·0713	0·00933	−0·0716	0·0060	−0·00221	1·5465	
−2·14	−0·0572	0·00872	−0·0575	0·0060	−0·00203	1·5396	
−1·63	−0·0445	0·00801	−0·0447	0·0067	−0·00164	1·5763	
−1·11	−0·0327	0·00611	−0·0329	0·0055	−0·00001	1·6897	
−0·60	−0·0192	0·00591	−0·0192	0·0057	0·00003	1·8370	
−0·08	−0·0003	0·00577	−0·0003	0·0058	0·00001	—	
0·43	0·0123	0·00574	0·0124	0·0056	−0·00006	1·6350	
0·95	0·0308	0·00584	0·0309	0·0053	−0·00011	1·8593	
1·46	0·0411	0·00703	0·0413	0·0060	0·00113	1·6158	
1·97	0·0523	0·00839	0·0526	0·0066	0·00195	1·5260	
2·49	0·0701	0·00920	0·0705	0·0061	0·00217	1·6197	
3·01	0·0842	0·01002	0·0846	0·0056	0·00229	1·6113	1·3116
3·53	0·1040	0·01145	0·1046	0·0050	0·00204	1·6977	1·3881
4·05	0·1205	0·01274	0·1211	0·0042	0·00179	1·7157	1·3918
4·57	0·1437	0·01483	0·1455	0·0033	0·00133	1·8113	1·3840
5·09	0·1609	0·01697	0·1617	0·0026	0·00122	1·8215	1·4372
5·65	0·1678	0·01972	0·1689	0·0031	0·00263	1·7142	1·7130
10·84	0·4006	0·06683	0·4061	−0·0097	−0·00175	2·1467	1·4778
16·09	0·6432	0·16156	0·6627	−0·0231	−0·00268	2·3596	1·4923
21·37	0·9014	0·31379	0·9537	−0·0362	−0·00573	2·5577	1·5114

TABLE 5 (Contd)

Gothic Wing, A = 1·277, x_t/c = 0·423, Transition Fixed at Leading Edge

α, deg	C_L	C_D	C_N	C_A	C_m	C_N/α	K
−4·79	−0·1527	0·01834	−0·1537	0·0055	−0·00076	1·8392	
−4·22	−0·1295	0·01590	−0·1303	0·0063	−0·00130	1·7718	
−3·70	−0·1129	0·01443	−0·1136	0·0071	−0·00164	1·7604	C_{D_0} =
−3·18	−0·0931	0·01308	−0·0937	0·0079	−0·00151	1·6900	0·0101
−2·66	−0·0786	0·01221	−0·0791	0·0085	−0·00147	1·7029	
−2·14	−0·0604	0·01138	−0·0608	0·0091	−0·00109	1·6258	
−1·63	−0·0473	0·01092	−0·0476	0·0096	−0·00086	1·6743	
−1·12	−0·0343	0·01057	−0·0345	0·0099	−0·00062	1·7716	
−0·60	−0·0166	0·01041	−0·0167	0·0102	−0·00033	1·6014	
−0·08	−0·0026	0·01032	−0·0026	0·0103	0·00005	1·7808	
0·43	0·0099	0·01029	0·0100	0·0102	0·00044	1·3330	
0·95	0·0273	0·01051	0·0275	0·0101	0·00060	1·6595	
1·46	0·0402	0·01061	0·0404	0·0096	0·00087	1·5852	
1·98	0·0584	0·01133	0·0588	0·0093	0·00102	1·7004	
2·50	0·0724	0·01168	0·0729	0·0085	0·00133	1·6731	
3·01	0·0908	0·01271	0·0913	0·0079	0·00131	1·7359	1·318
3·53	0·1053	0·01351	0·1059	0·0070	0·00152	1·7190	1·270
4·05	0·1221	0·01492	0·1228	0·0063	0·00135	1·7387	1·325
4·57	0·1437	0·01700	0·1446	0·0055	0·00085	1·8132	1·360
5·09	0·1608	0·01903	0·1619	0·0047	0·00063	1·8233	1·400
5·61	0·1839	0·02190	0·1852	0·0038	0·00025	1·8907	1·411
6·65	0·2197	0·02712	0·2214	0·0015	0·00008	1·9078	1·423
7·70	0·2650	0·03530	0·2673	−0·0005	−0·00037	1·9901	1·445
8·75	0·3111	0·04523	0·3143	−0·0026	−0·00078	2·0597	1·460
9·79	0·3559	0·05647	0·3603	−0·0049	−0·00146	2·1085	1·471
10·84	0·4037	0·06989	0·4096	−0·0073	−0·00157	2·1648	1·475
11·89	0·4472	0·08375	0·4549	−0·0102	−0·00189	2·1926	1·479
12·94	0·4973	0·10120	0·5073	−0·0127	−0·00216	2·2465	1·479
13·99	0·5403	0·11797	0·5528	−0·0161	−0·00205	2·2651	1·484
15·04	0·5892	0·13837	0·6049	−0·0192	−0·00194	2·3051	1·483
16·08	0·6638	0·15907	0·6531	−0·0228	−0·00208	2·3267	1·489
17·14	0·6881	0·18592	0·7123	−0·0251	−0·00301	2·3812	1·491
18·19	0·7364	0·21215	0·7658	−0·0283	−0·00368	2·4121	1·495
19·30	0·7950	0·24583	0·8316	−0·0308	−0·00459	2·4683	1·497
20·29	0·8431	0·27581	0·8870	−0·0326	−0·00550	2·5041	1·499
21·36	0·8941	0·31137	0·9461	−0·0357	−0·00550	2·5381	1·512
22·41	0·9417	0·34595	1·0025	−0·0392	−0·00619	2·5634	1·520
23·46	0·9902	0·38303	1·0609	−0·0429	−0·00691	2·5910	1·526
24·51	1·0405	0·42376	1·1125	−0·0462	−0·00798	2·6238	1·533
25·56	1·0874	0·46642	1·1823	−0·0485	−0·00847	2·6498	1·549
26·61	1·1315	0·50986	1·2400	−0·0510	−0·00947	2·6699	1·567

TABLE 6

Gothic Wing, A = 1·277, Φ/S = 0·075, Transition Free

α, deg	C_L	C_D	C_N	C_A	C_m	C_N/α	K
−4·57	−0·1492	0·01721	−0·1501	0·0053	−0·00142	1·884	
−4·05	−0·1322	0·01524	−0·1330	0·0059	−0·00134	1·882	C_{D_0} =
−3·52	−0·1082	0·01280	−0·1085	0·0061	−0·00155	1·769	0·0081
−3·00	−0·0902	0·01110	−0·0906	0·0064	−0·00163	1·729	
−2·48	−0·0679	0·00952	−0·0682	0·0066	−0·00184	1·575	
−1·97	−0·0532	0·00882	−0·0535	0·0070	−0·00173	1·560	
−1·45	−0·0408	0·00804	−0·0410	0·0070	−0·00120	1·616	
−0·94	−0·0285	0·00712	−0·0286	0·0067	−0·00106	1·742	
−0·42	−0·0116	0·00649	−0·0117	0·0064	−0·00036	1·582	
0·09	0·0019	0·00632	0·0020	0·0063	0·00004	1·219	
0·61	0·0154	0·00621	0·0154	0·0060	0·00086	1·459	
1·12	0·0333	0·00671	0·0334	0·0061	0·00125	1·703	
1·64	0·0442	0·00801	0·0444	0·0067	0·00192	1·556	
2·15	0·0621	0·00906	0·0624	0·0067	0·00215	1·659	
2·67	0·0767	0·00994	0·0771	0·0064	0·00239	1·655	
3·19	0·0990	0·01155	0·0995	0·0060	0·00205	1·785	
3·71	0·1176	0·01342	0·1182	0·0058	0·00193	1·824	1·543
4·23	0·1354	0·01517	0·1361	0·0051	0·00176	1·843	1·547
4·75	0·1528	0·01706	0·1537	0·0043	0·00168	1·854	1·538
5·27	0·1704	0·01924	0·1714	0·0035	0·00144	1·865	1·539
5·79	0·1948	0·02274	0·1961	0·0030	0·00116	1·940	1·537
6·84	0·2354	0·02910	0·2372	0·0009	0·00080	1·988	1·520
7·88	0·2812	0·03803	0·2838	−0·0009	0·00013	2·062	1·518
8·93	0·3283	0·04855	0·3318	−0·0030	−0·00041	2·128	1·506
9·98	0·3727	0·05974	0·3774	−0·0058	−0·00136	2·167	1·491
11·02	0·4153	0·07170	0·4214	−0·0090	−0·00187	2·190	1·479
12·08	0·4654	0·08744	0·4725	−0·0117	−0·00196	2·242	1·475
13·12	0·5086	0·10290	0·5187	−0·0152	−0·00181	2·265	1·470
14·17	0·5575	0·12203	0·5705	−0·0182	−0·00265	2·306	1·470
15·22	0·6025	0·14072	0·6183	−0·0224	−0·00361	2·327	1·466
16·28	0·6556	0·16477	0·6755	−0·0256	−0·00389	2·378	1·462
17·33	0·7043	0·18865	0·7285	−0·0297	−0·00446	2·409	1·460
18·38	0·7531	0·21463	0·7824	−0·0338	−0·00490	2·439	1·461
19·43	0·8026	0·24318	0·8378	−0·0377	−0·00557	2·470	1·464
20·50	0·8638	0·28157	0·9077	−0·0387	−0·00697	2·537	1·470
21·55	0·9121	0·31528	0·9641	−0·0417	−0·00807	2·564	1·481
22·60	0·9655	0·35530	1·0279	−0·0431	−0·00928	2·605	1·494
23·65	1·0126	0·39370	1·0855	−0·0457	−0·01038	2·629	1·509
24·71	1·0660	0·43940	1·1521	−0·0465	−0·01118	2·671	1·523
25·77	1·1161	0·48432	1·2157	−0·0490	−0·01105	2·703	1·534
26·82	1·1674	0·53171	1·2817	−0·0522	−0·01188	2·738	1·541

TABLE 6 (Contd)

Gothic Wing, A = 1·277, Φ/S = 0·075, Transition Fixed at Shoulder

α, deg	C_L	C_D	C_N	C_A	C_m	C_N/α	K
0·60	0·0125	0·00754	0·0126	0·0074	0·00051	1·193	C_{D_0} =
1·64	0·0433	0·01249	0·0436	0·0112	0·00102	1·529	0·0087
2·67	0·0765	0·01047	0·0769	0·0069	0·00165	1·651	
3·71	0·1168	0·01391	0·1175	0·0063	0·00135	1·813	1·533
4·75	0·1551	0·01795	0·1561	0·0050	0·00124	1·882	1·543
5·80	0·1965	0·02366	0·1979	0·0037	0·00089	1·957	1·554
6·83	0·2334	0·02967	0·2352	0·0017	0·00067	1·972	1·544
7·88	0·2760	0·03774	0·2785	−0·0004	0·00019	2·026	1·530
8·93	0·3234	0·04817	0·3270	−0·0026	−0·00063	2·098	1·514
9·98	0·3712	0·06054	0·3760	−0·0047	−0·00097	2·159	1·510
11·03	0·4161	0·07365	0·4225	−0·0073	−0·00135	2·196	1·505
12·07	0·4609	0·08843	0·4692	−0·0099	−0·00152	2·227	1·506
13·12	0·5094	0·10736	0·5204	−0·0111	−0·00215	2·272	1·526
14·17	0·5533	0·12443	0·5669	−0·0148	−0·00258	2·293	1·516
15·22	0·6054	0·14463	0·6221	−0·0194	−0·00288	2·341	1·488
16·27	0·6517	0·16581	0·6720	−0·0234	−0·00353	2·366	1·484
17·32	0·7002	0·18912	0·7248	−0·0280	−0·00393	2·397	1·476
18·38	0·7513	0·21631	0·7812	−0·0316	−0·00488	2·436	1·476
19·43	0·8008	0·24442	0·8365	−0·0359	−0·00580	2·467	1·475
20·48	0·8510	0·27508	0·8934	−0·0401	−0·00627	2·499	1·476
21·53	0·8998	0·30674	0·9496	−0·0450	−0·00696	2·526	1·477
21·54	0·9063	0·31112	0·9572	−0·0434	−0·00674	2·546	1·477
22·60	0·9642	0·35284	1·0258	−0·0449	−0·00809	2·600	1·485
23·66	1·0130	0·39009	1·0844	−0·0491	−0·00928	2·627	1·491
24·72	1·0711	0·43935	1·1567	−0·0488	−0·01054	2·681	1·506
25·76	1·1112	0·47698	1·2081	−0·0534	−0·01133	2·687	1·521
26·82	1·1654	0·53302	1·2805	−0·0501	−0·01328	2·736	1·549

TABLE 7

Gothic Wing, A = 1·277, x_t/c = 0·333, Transition Free

α, deg	C_L	C_D	C_N	C_A	C_m	C_N/α	K
−4·65	−0·1502	0·01589	−0·1510	0·0037	0·00056	1·8615	
−4·13	−0·1373	0·01369	−0·1380	0·0038	0·00084	1·9126	C_{D_0} =
−3·61	−0·1192	0·01249	−0·1197	0·0049	0·00029	1·8982	0·0080
−3·10	−0·1044	0·01116	−0·1048	0·0055	0·00094	1·9379	
−2·57	−0·0800	0·01027	−0·0804	0·0067	−0·00036	1·7895	
−2·05	−0·0618	0·00911	−0·0621	0·0069	−0·00029	1·7313	
−1·54	−0·0486	0·00797	−0·0488	0·0067	−0·00046	1·8164	
−1·02	−0·0311	0·00725	−0·0312	0·0067	−0·00028	1·7473	
−0·50	−0·0126	0·00708	−0·0127	0·0070	−0·00015	1·4416	
0·01	+0·0008	0·00690	0·0008	0·0069	0·00060	—	
0·53	0·0158	0·00698	0·0159	0·0068	0·00018	1·7283	
1·05	0·0339	0·00730	0·0341	0·0067	0·00067	1·8673	
1·56	0·0515	0·00772	0·0517	0·0063	0·00067	1·8941	
2·08	0·0643	0·00870	0·0646	0·0064	0·00079	1·7821	
2·59	0·0783	0·00975	0·0786	0·0062	0·00084	1·7380	
3·11	0·0923	0·01067	0·0928	0·0056	0·00075	1·7111	1·245
3·63	0·1111	0·01183	0·1116	0·0048	0·00083	1·7636	1·245
4·15	0·1299	0·01334	0·1306	0·0039	0·00091	1·8046	1·269
4·66	0·1473	0·01502	0·1480	0·0030	0·00047	1·8185	1·298
5·18	0·1639	0·01681	0·1647	0·0019	0·00004	1·8217	1·316
5·70	0·1856	0·01959	0·1866	0·0010	−0·00046	1·8747	1·350

TABLE 7 (Contd)

Gothic Wing, A = 1·277, x_t/c = 0·333, Transition Fixed at Leading Edge

α, deg	C_L	C_D	C_N	C_A	C_m	C_N/α	K
−4·65	−0·1493	0·01744	−0·1503	0·0053	−0·00006	1·8523	
−4·12	−0·1285	0·01548	−0·1293	0·0062	−0·00048	1·7965	C_{D_0} =
−3·60	−0·1088	0·01390	−0·1095	0·0070	−0·00069	1·7407	0·0100
−3·09	−0·0943	0·01294	−0·0949	0·0078	−0·00059	1·7601	
−2·57	−0·0805	0·01226	−0·0809	0·0086	−0·00044	1·8018	
−2·05	−0·0620	0·01137	−0·0623	0·0091	−0·00027	1·7379	
−1·54	−0·0488	0·01112	−0·0491	0·0098	−0·00020	1·8248	
−1·02	−0·0304	0·01062	−0·0306	0·0101	−0·00010	1·7172	
−0·51	−0·0169	0·01037	−0·0170	0·0102	−0·00008	1·9209	
−0·04	−0·0040	0·01037	−0·0040	0·0104	0·00030	—	
0·52	0·0143	0·01034	0·0144	0·0102	−0·00007	1·5754	
1·04	0·0314	0·01060	0·0316	0·0100	0·00012	1·7375	
1·56	0·0494	0·01104	0·0497	0·0097	0·00024	1·8226	
2·08	0·0675	0·01157	0·0679	0·0091	0·00036	1·8693	
2·59	0·0808	0·01212	0·0812	0·0085	0·00048	1·7942	
3·11	0·0958	0·01300	0·0964	0·0078	0·00056	1·7752	1·310
3·62	0·1090	0·01366	0·1097	0·0067	0·00084	1·7344	1·235
4·14	0·1285	0·01504	0·1293	0·0057	0·00074	1·7877	1·223
4·67	0·1494	0·01706	0·1503	0·0048	0·00053	1·8458	1·268
5·18	0·1650	0·01874	0·1660	0·0038	0·00031	1·8357	1·287
71	0·1896	0·02179	0·1909	0·0028	−0·00024	1·9152	1·316
6·76	0·2255	0·02711	0·2276	0·0025	−0·00085	1·9272	1·377
7·80	0·2748	0·03602	0·2772	−0·0016	−0·00200	2·0368	1·382
8·89	0·3184	0·04549	0·3216	−0·0043	−0·00274	2·0721	1·405
9·89	0·3592	0·05556	0·3634	−0·0069	−0·00347	2·1065	1·416
10·94	0·4077	0·06815	0·4132	−0·0104	−0·00434	2·1650	1·404
11·99	0·4566	0·08319	0·4639	−0·0135	−0·00525	2·2176	1·408
13·04	0·5065	0·10045	0·5161	−0·0164	−0·00601	2·2677	1·414
14·09	0·5559	0·11917	0·5682	−0·0198	−0·00621	2·3105	1·417
15·14	0·6045	0·13958	0·6200	−0·0232	−0·00675	2·3460	1·422
16·20	0·6548	0·16300	0·6743	−0·0261	−0·00692	2·3857	1·432
17·25	0·7038	0·18655	0·7275	−0·0305	−0·00825	2·4169	1·430
18·30	0·7513	0·21260	0·7800	−0·0340	−0·00925	2·4427	1·440
19·36	0·8072	0·24512	0·8428	−0·0363	−0·01035	2·4948	1·448
20·40	0·8512	0·27287	0·8930	−0·0410	−0·01096	2·5078	1·455
21·46	0·9071	0·30947	0·9575	−0·0439	−0·01194	2·5562	1·460
22·52	0·9630	0·35044	1·0238	−0·0451	−0·01283	2·6047	1·473
23·57	1·0109	0·38725	1·0814	−0·0493	−0·01381	2·6287	1·481
24·63	1·0658	0·43309	1·1493	−0·0505	−0·01619	2·6737	1·494
25·67	1·1061	0·46950	1·2003	−0·0561	−0·01640	2·6788	1·507
26·73	1·1559	0·51630	1·2646	−0·0587	−0·01755	2·7111	1·521

TABLE 8

Gothic Wing, A = 1·456, x_t/c = 0·250, Transition Free

α, deg	C_L	C_D	C_N	C_A	C_m	C_N/α	K
−4·03	−0·1462	0·01462	−0·1469	0·0043	0·00035	2·089	
−3·61	−0·1285	0·01297	−0·1290	0·0048	0·00005	2·045	
−3·20	−0·1111	0·01155	−0·1116	0·0053	−0·00033	1·999	
−2·68	−0·0939	0·01030	−0·0942	0·0059	−0·00044	2·012	
−2·22	−0·0768	0·00925	−0·0771	0·0063	−0·00061	1·992	
−1·75	−0·0608	0·00852	−0·0610	0·0067	−0·00055	1·994	
−1·34	−0·0444	0·00783	−0·0446	0·0069	−0·00050	1·906	
−0·82	−0·0279	0·00764	−0·0281	0·0072	−0·00027	1·948	
−0·36	−0·0120	0·00733	−0·0120	0·0073	−0·00011	1·909	
0·15	0·0038	0·00723	0·0038	0·0072	0·00006	—	
0·62	0·0193	0·00732	0·0193	0·0071	0·00039	1·795	
1·08	0·0362	0·00760	0·0364	0·0069	0·00064	1·926	
1·50	0·0525	0·00803	0·0527	0·0067	0·00061	2·016	
1·96	0·0679	0·00874	0·0682	0·0064	0·00066	1·993	
2·43	0·0852	0·00970	0·0855	0·0061	0·00054	2·020	
2·94	0·1022	0·01076	0·1026	0·0057	0·00034	2·000	
3·41	0·1197	0·01189	0·1201	0·0050	0·00019	2·021	
3·87	0·1369	0·01330	0·1375	0·0043	0·00004	2·032	
4·34	0·1549	0·01487	0·1556	0·0034	−0·00004	2·058	

TABLE 8 (Contd)

Gothic Wing, A = 1·456, x_t/c = 0·250, Transition Free

α, deg	C_L	C_D	C_N	C_A	C_m	C_N/α	K
−3·51	−0·1243	0·01280	−0·1249	0·0054	0·00022	2·098	
−2·37	−0·0838	0·00980	−0·0841	0·0063	−0·00082	2·029	C_{D_0} =
−1·24	−0·0411	0·00798	−0·0412	0·0071	−0·00134	1·911	0·0076
−0·21	−0·0079	0·00730	−0·0079	0·0073	−0·00006	2·192	
+0·83	0·0290	0·00736	0·0291	0·0069	0·00058	2·017	
1·96	0·0682	0·00871	0·0684	0·0064	0·00062	2·000	
3·09	0·1059	0·01099	0·1064	0·0053	0·00062	1·970	
4·23	0·1469	0·01409	0·1476	0·0032	0·00027	1·999	1·374
5·17	0·1903	0·01843	0·1912	0·0005	−0·00017	2·119	1·368
6·31	0·2359	0·02430	0·2372	−0·0026	−0·00085	2·152	1·372
7·45	0·2856	0·03220	0·2873	−0·0061	−0·00186	2·209	1·380
8·75	0·3420	0·04328	0·3446	−0·0096	−0·00275	2·252	1·395
9·95	0·3951	0·05406	0·3985	−0·0150	−0·00359	2·294	1·361
11·10	0·4461	0·06876	0·4507	−0·0201	−0·00401	2·327	1·401
12·24	0·4962	0·08436	0·5028	−0·0228	−0·00408	2·353	1·426
13·39	0·5514	0·10325	0·5603	−0·0273	−0·00553	2·397	1·439
14·65	0·6131	0·12574	0·6250	−0·0334	−0·00728	2·445	1·438
15·80	0·6742	0·15131	0·6900	−0·0380	−0·00900	2·502	1·446
16·96	0·7345	0·17911	0·7549	−0·0416	−0·01044	2·550	1·454
18·11	0·7934	0·20917	0·8191	−0·0478	−0·01185	2·592	1·465
19·16	0·8514	0·24199	0·8836	−0·0508	−0·01357	2·642	1·479
20·42	0·9149	0·28100	0·9554	−0·0558	−0·01565	2·681	1·494
21·57	0·9715	0·31993	1·0211	−0·0596	−0·01702	2·712	1·514
22·82	1·0301	0·36314	1·0903	−0·0649	−0·01962	2·737	1·533
24·07	1·0896	0·41120	1·1625	−0·0691	−0·02210	2·767	1·555
25·33	1·1469	0·46145	1·2341	−0·0736	−0·02518	2·792	1·578
26·58	1·2004	0·51446	1·3037	−0·0770	−0·02801	2·811	1·609

TABLE 9
Linear and Non-Linear Normal Force Components

Planform	A	$\frac{x_r}{c}$	$\frac{\Phi}{S}$	$A\left(1+\frac{c_{0\cdot99}}{c}\right)$	η	α, deg	$\frac{\alpha}{A}$	$\frac{C_N}{\alpha}$	$\Delta\left(\frac{C_N}{\alpha}\right)$
Delta (Ref. 3)	1·456	0·423	0·08	1·470	0·636	0	0	1·50	0
						4	0·048	1·72	0·22
						8	0·096	1·94	0·44
						12	0·144	2·12	0·62
						16	0·192	2·28	0·78
						20	0·240	2·42	0·92
						24	0·288	2·54	1·04
Mild Gothic	1·456	0·423	0·08	1·555	0·704	0	0	1·67	0
						4	0·048	1·90	0·23
						8	0·096	2·13	0·46
						12	0·144	2·32	0·65
						16	0·192	2·44	0·77
						20	0·240	2·49	0·82
						24	0·288	2·60	0·93
Gothic	1·456	0·423	0·08	1·602	0·764	0	0	1·71	0
						4	0·048	1·94	0·23
						8	0·096	2·18	0·47
						12	0·144	2·36	0·65
						16	0·192	2·45	0·74
						20	0·240	2·61	0·90
						24	0·288	2·73	1·02
Gothic	1·277	0·423	0·08	1·405	0·820	0	0	1·53	0
						4	0·055	1·78	0·25
						8	0·109	2·01	0·48
						12	0·164	2·20	0·67
						16	0·218	2·33	0·80
						20	0·273	2·49	0·96
						24	0·328	2·61	1·07

TABLE 9 (Contd)
Linear and Non-Linear Normal Force Components

Planform	A	$\frac{x_t}{c}$	$\frac{\Phi}{S}$	$A\left(1+\frac{c_{0\cdot99}}{c}\right)$	η	α, deg	$\frac{\alpha}{A}$	$\frac{C_N}{\alpha}$	$\left(\frac{C_N}{\alpha}\right)$
Gothic	1·277	0·423	0·075	1·405	0·820	0	0	1·53	0
						4	0·055	1·82	0·29
						8	0·109	2·06	0·53
						12	0·162	2·23	0·70
						16	0·218	2·37	0·84
						20	0·273	2·50	0·97
						24	0·328	2·64	1·11
Gothic	1·277	0·333	0·08	1·405	0·820	0	0	1·60	0
						4	0·055	1·81	0·21
						8	0·109	2·01	0·41
						12	0·164	2·21	0·61
						16	0·218	2·37	0·77
						20	0·273	2·51	0·91
						24	0·328	2·65	1·05
Gothic	1·456	0·250	0·08	1·602	0·764	0	0	1·86	0
						4	0·048	2·05	0·19
						8	0·096	2·22	0·36
						12	0·144	2·35	0·49
						16	0·192	2·51	0·65
						20	0·240	2·67	0·81
						24	0·288	2·77	0·91

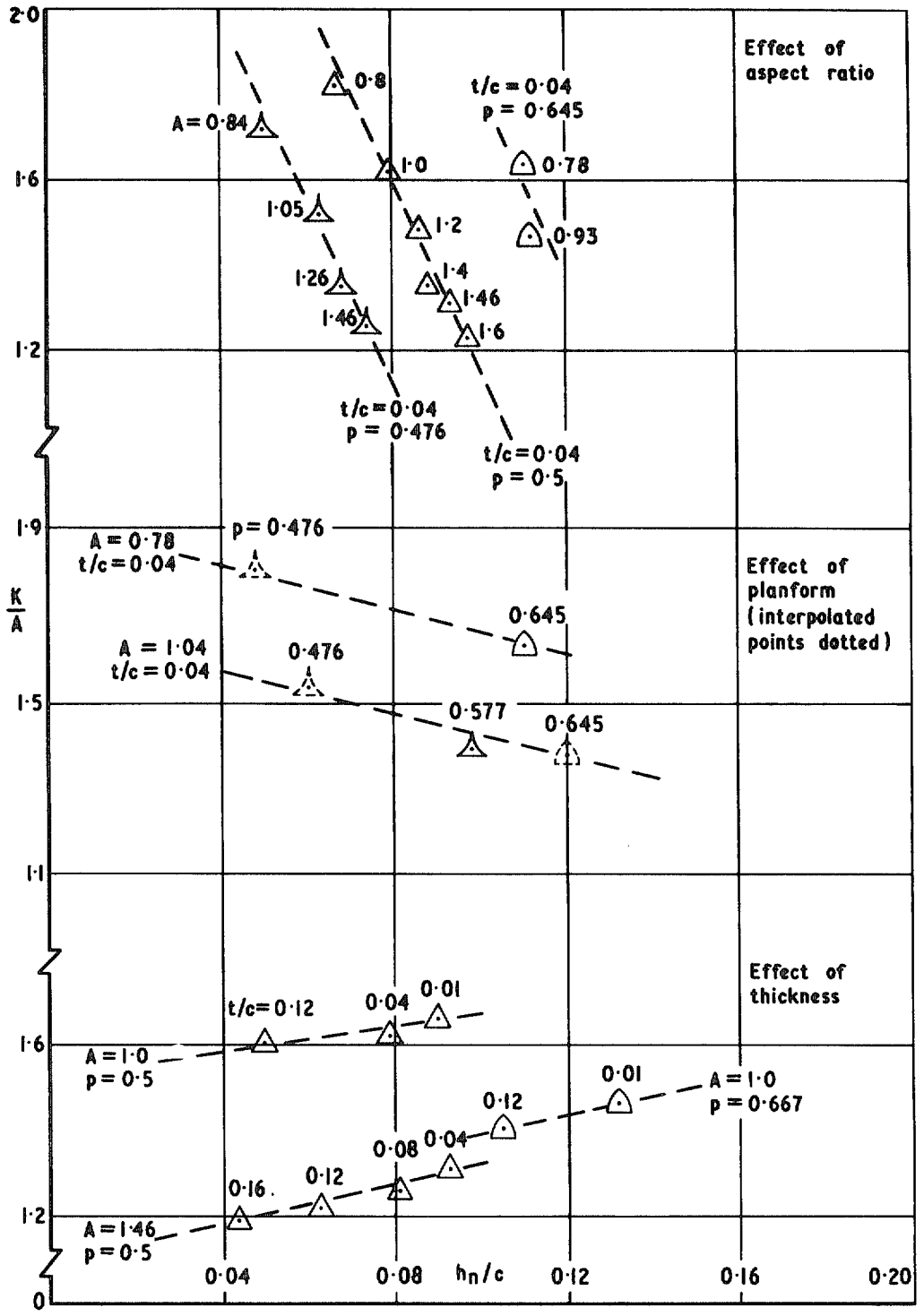

FIG. 1. Drag and stability of slender wings at $C_L = 0{\cdot}5$.

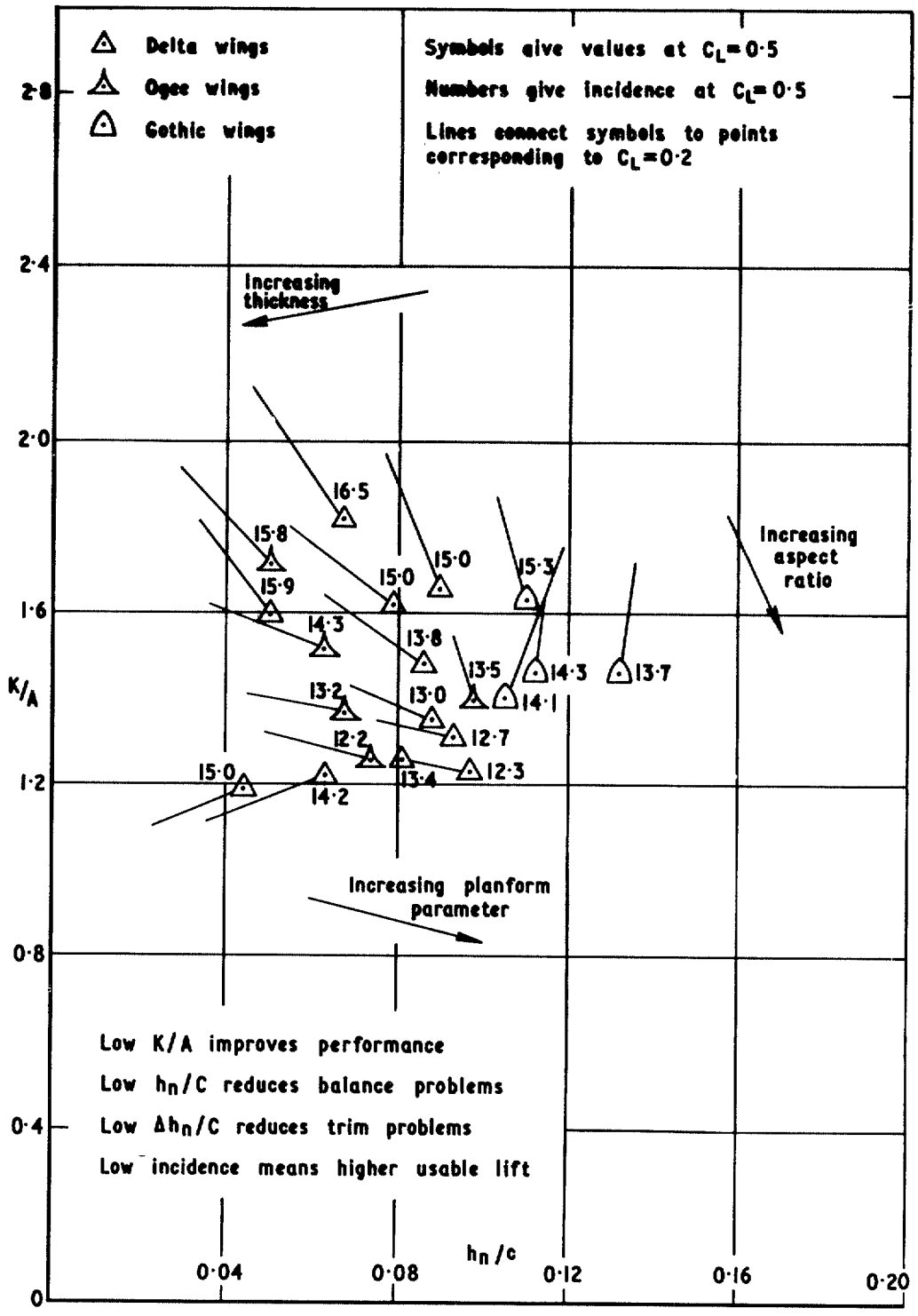

FIG. 2. Lift, drag and stability of slender wings.

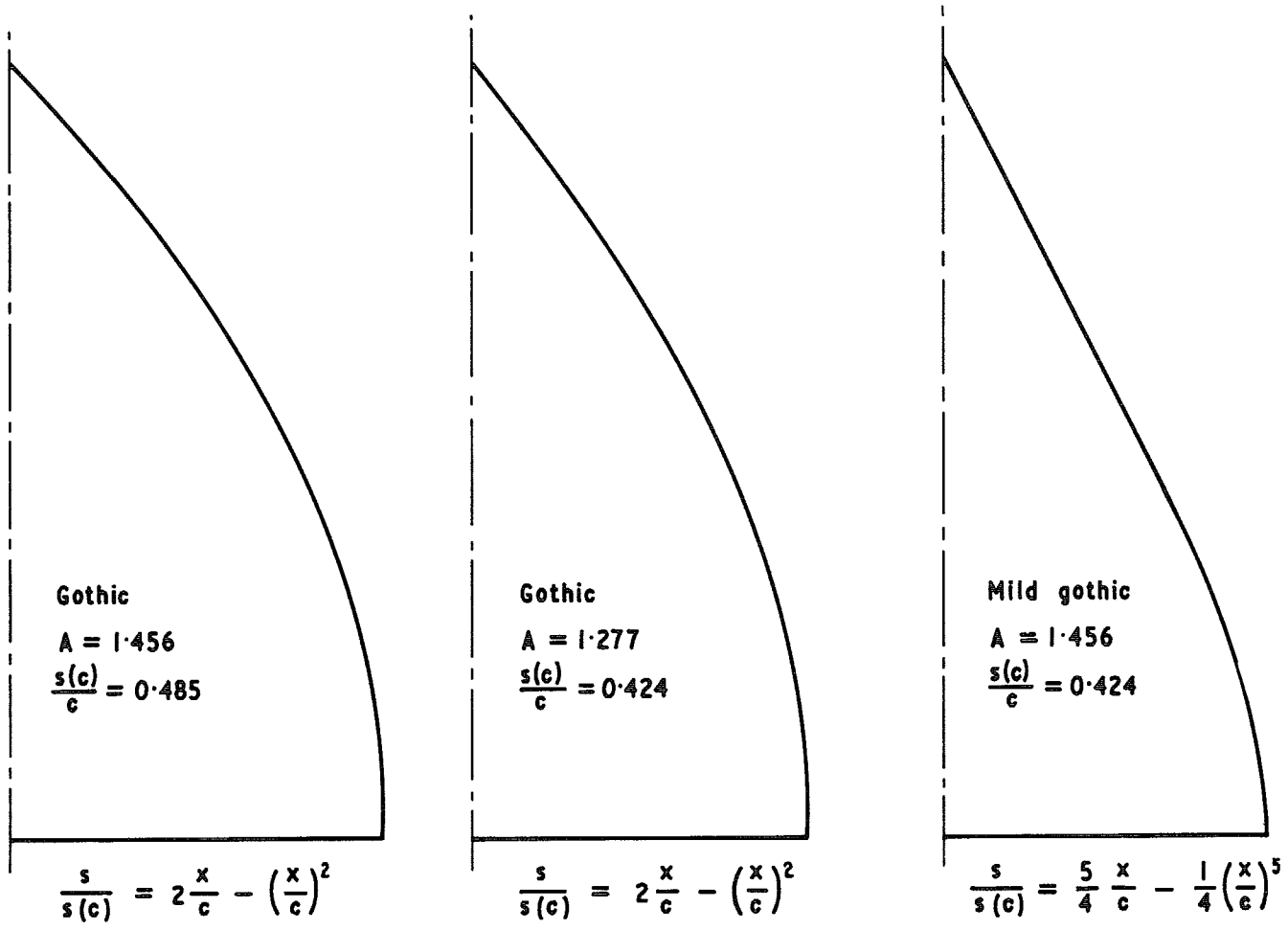

FIG. 3. Planforms of the wings tested.

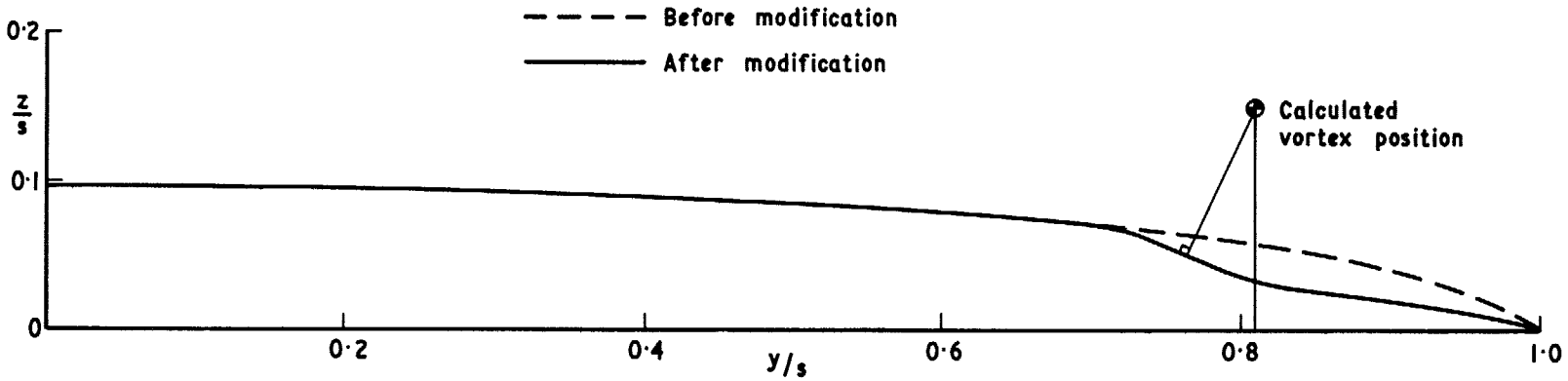

FIG. 4a. Spanwise cross-section at $x/c = 0{\cdot}6$ of gothic wing ($A = 1{\cdot}277$, $x_t/c = 0{\cdot}423$) before and after modification.

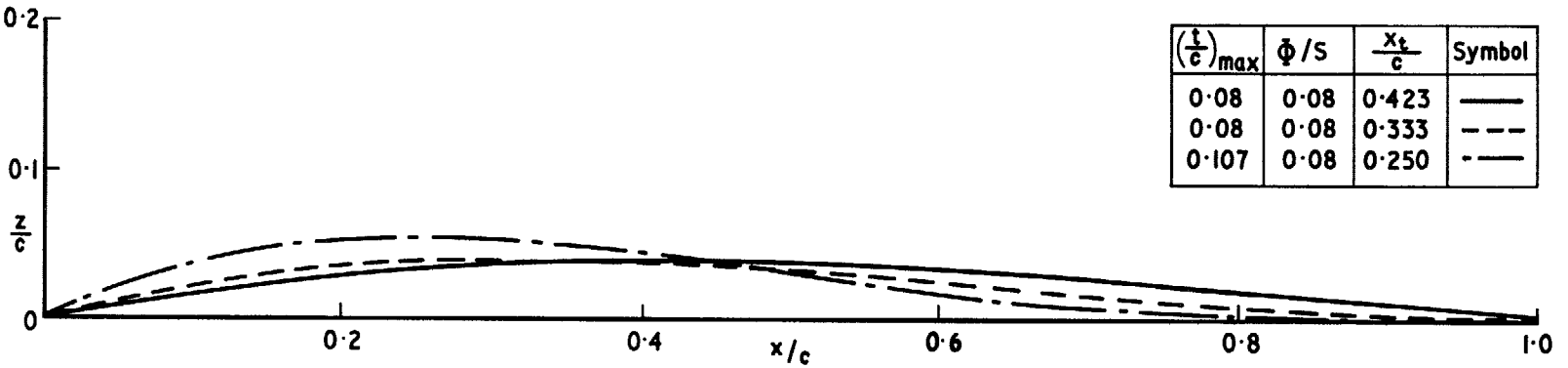

FIG. 4b. Chordwise sections at the centre lines of gothic wings.

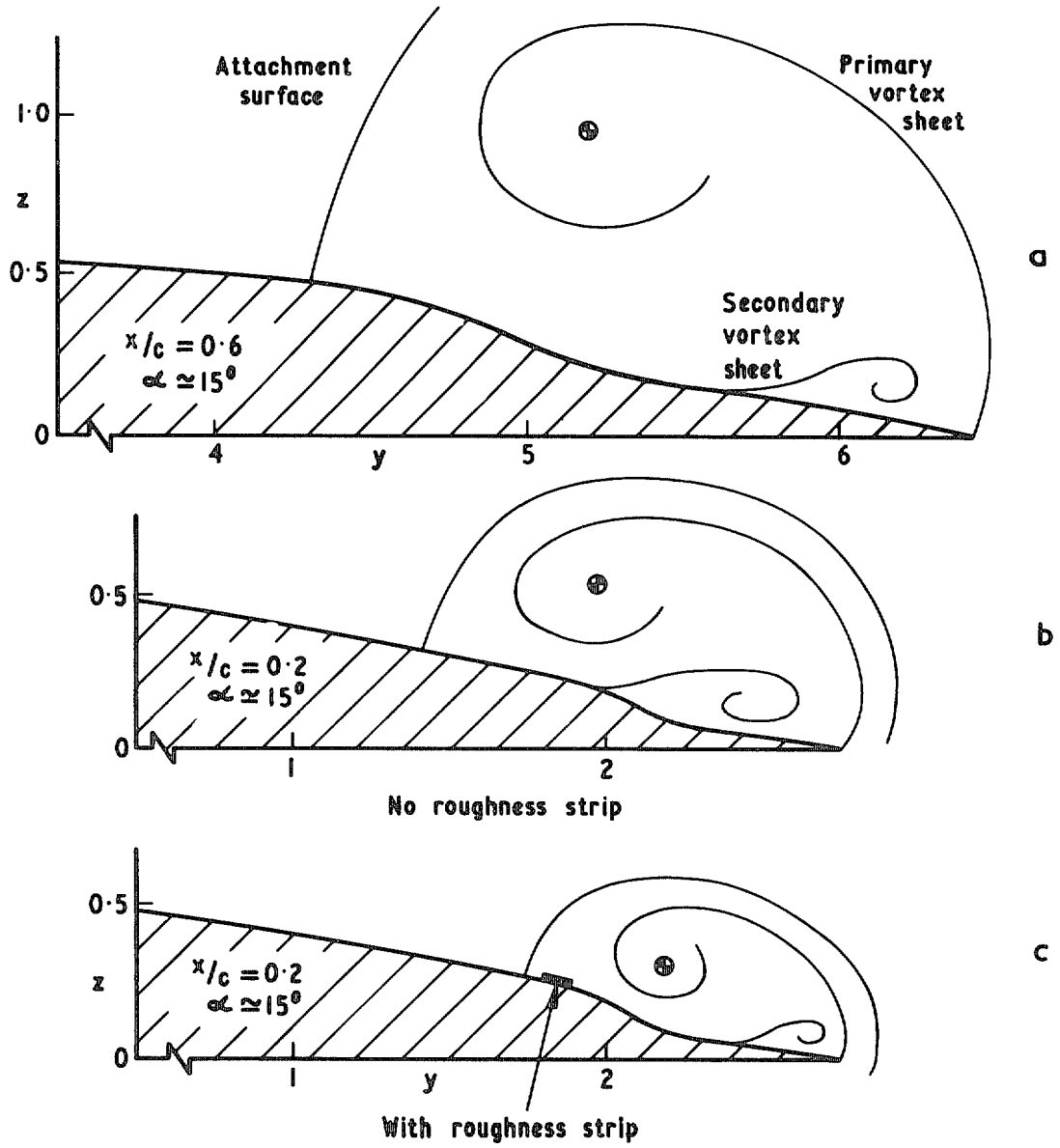

FIG. 5a c. Sketch of the spanwise cross-section of three-dimensional stream surfaces around wing B_2.

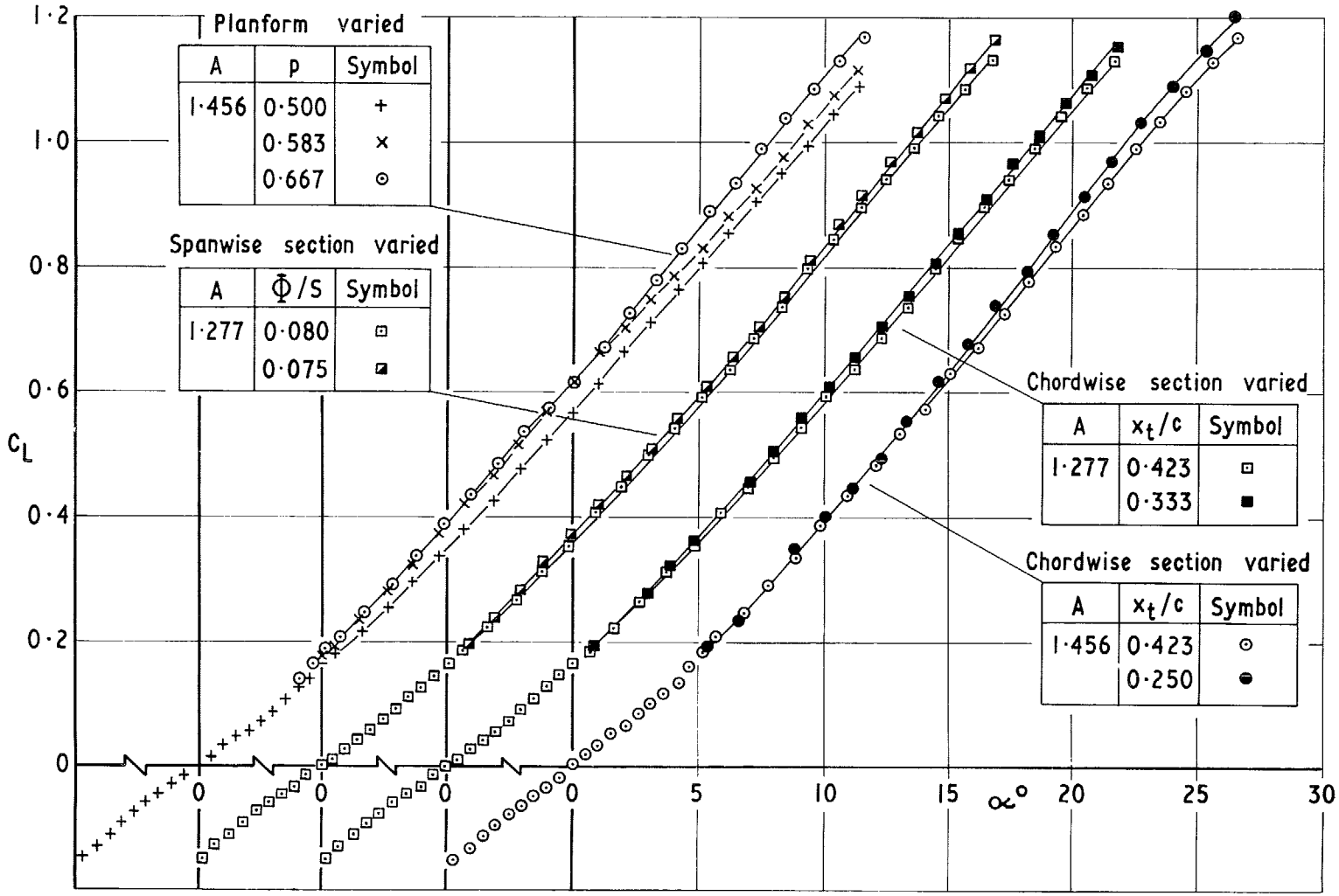

FIG. 6. Variation of lift coefficient with incidence.

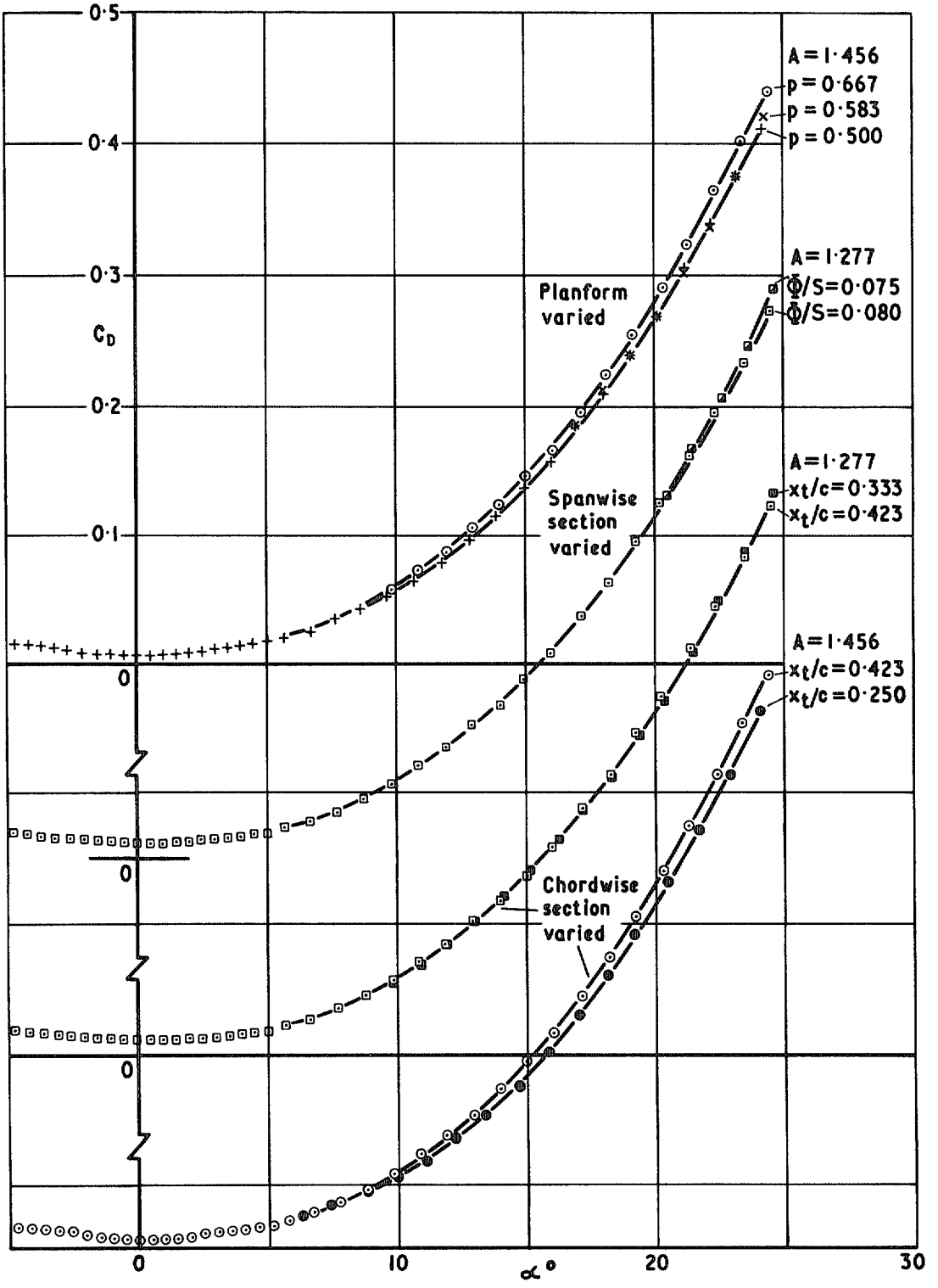

FIG. 7. Variation of drag coefficient with incidence.

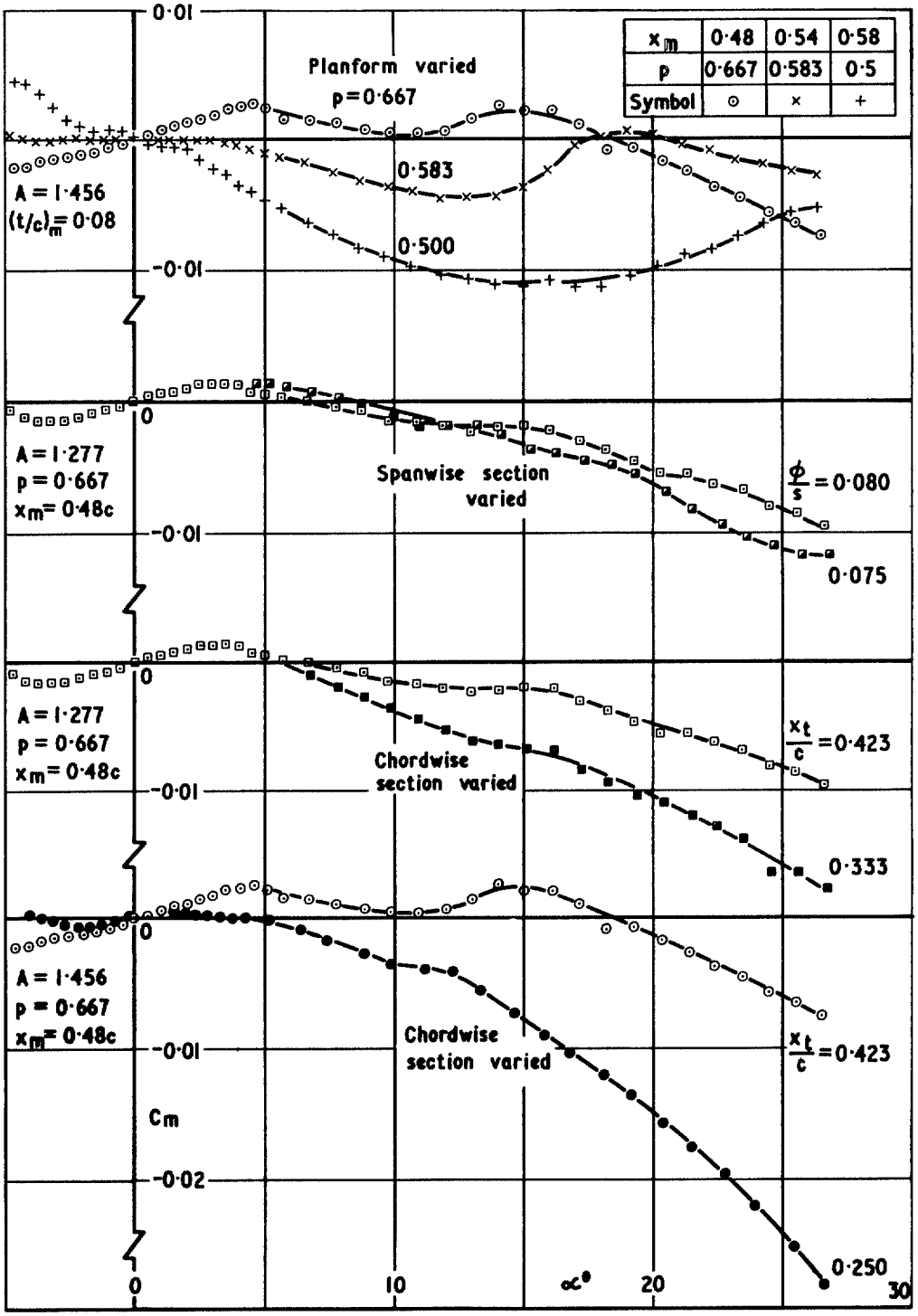

FIG. 8. Variation of pitching moment coefficient with incidence.

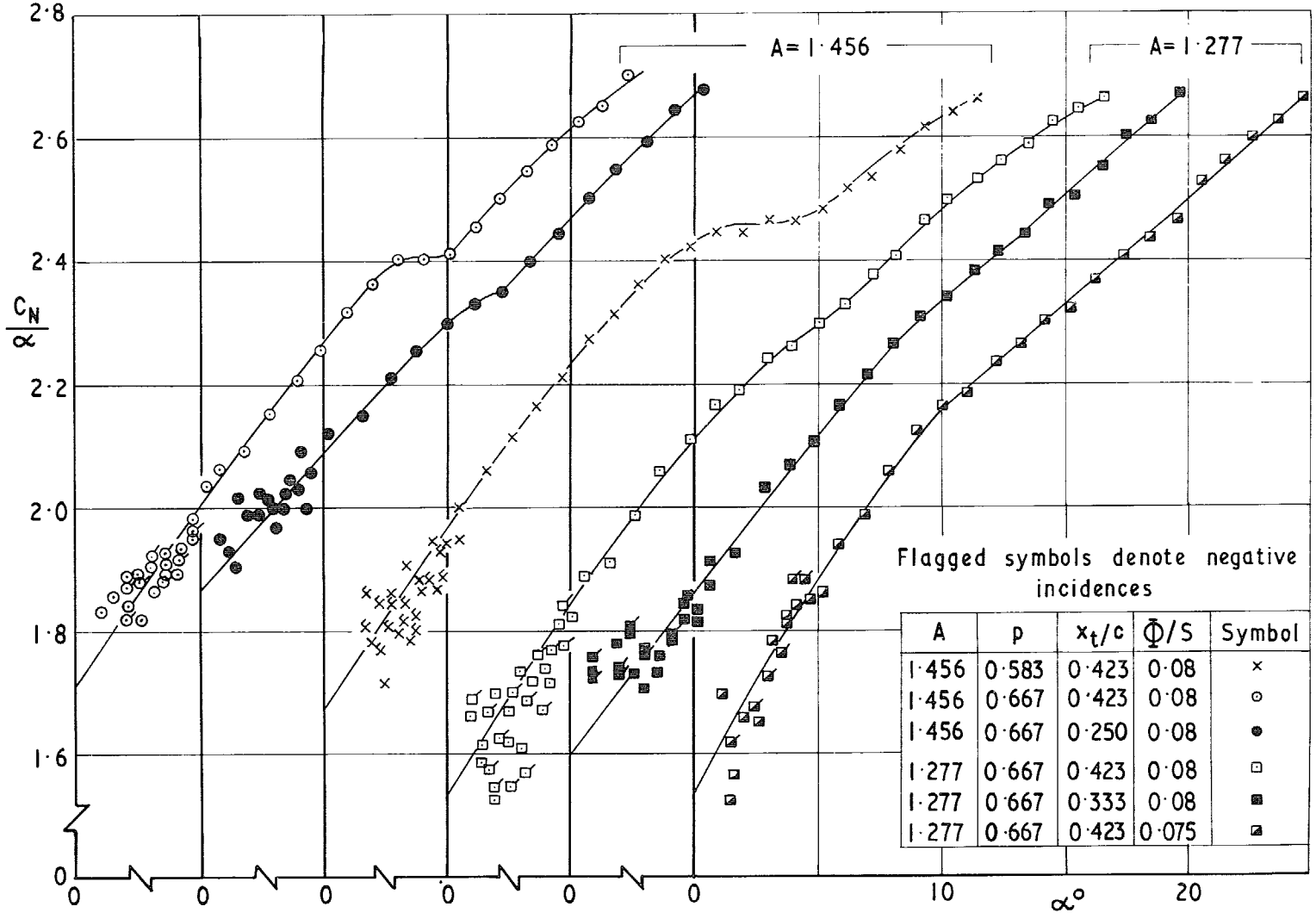

FIG. 9. Variation of C_N/α with incidence.

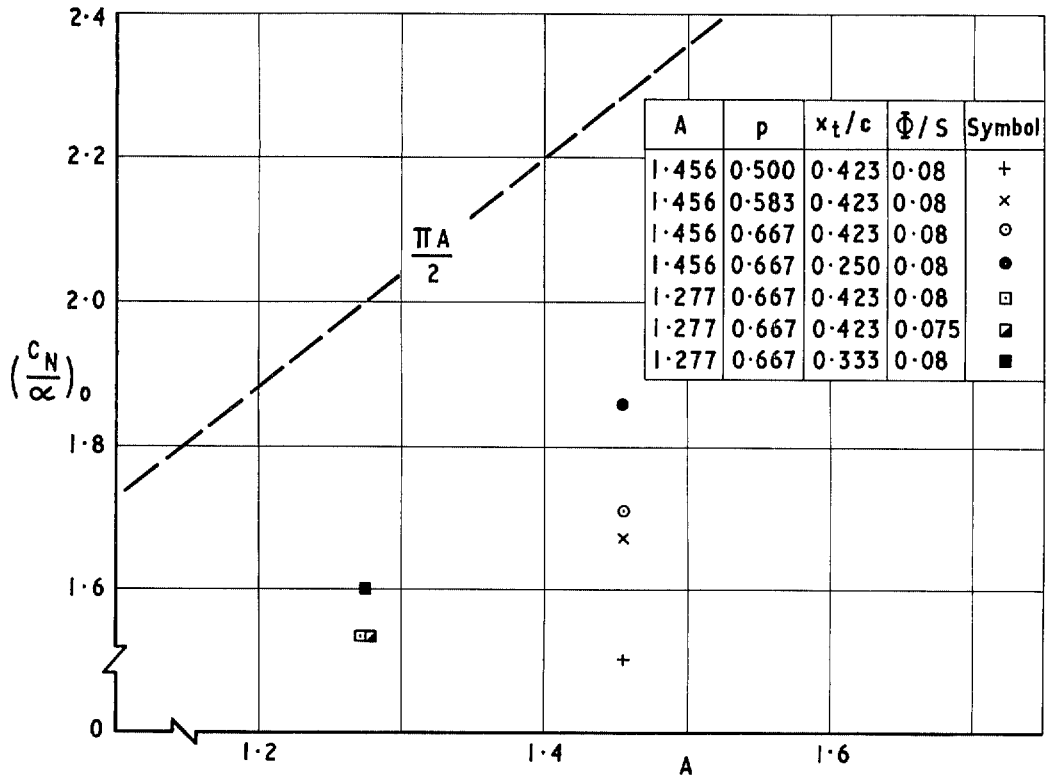

a. With aspect ratio

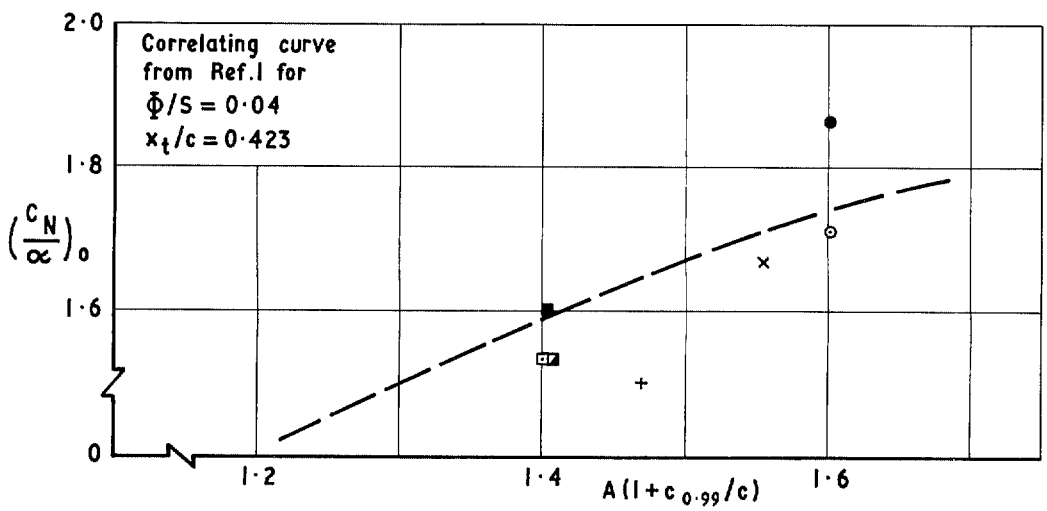

b. With modified aspect ratio parameter

FIG. 10 a & b. Variation of (C_N/α).

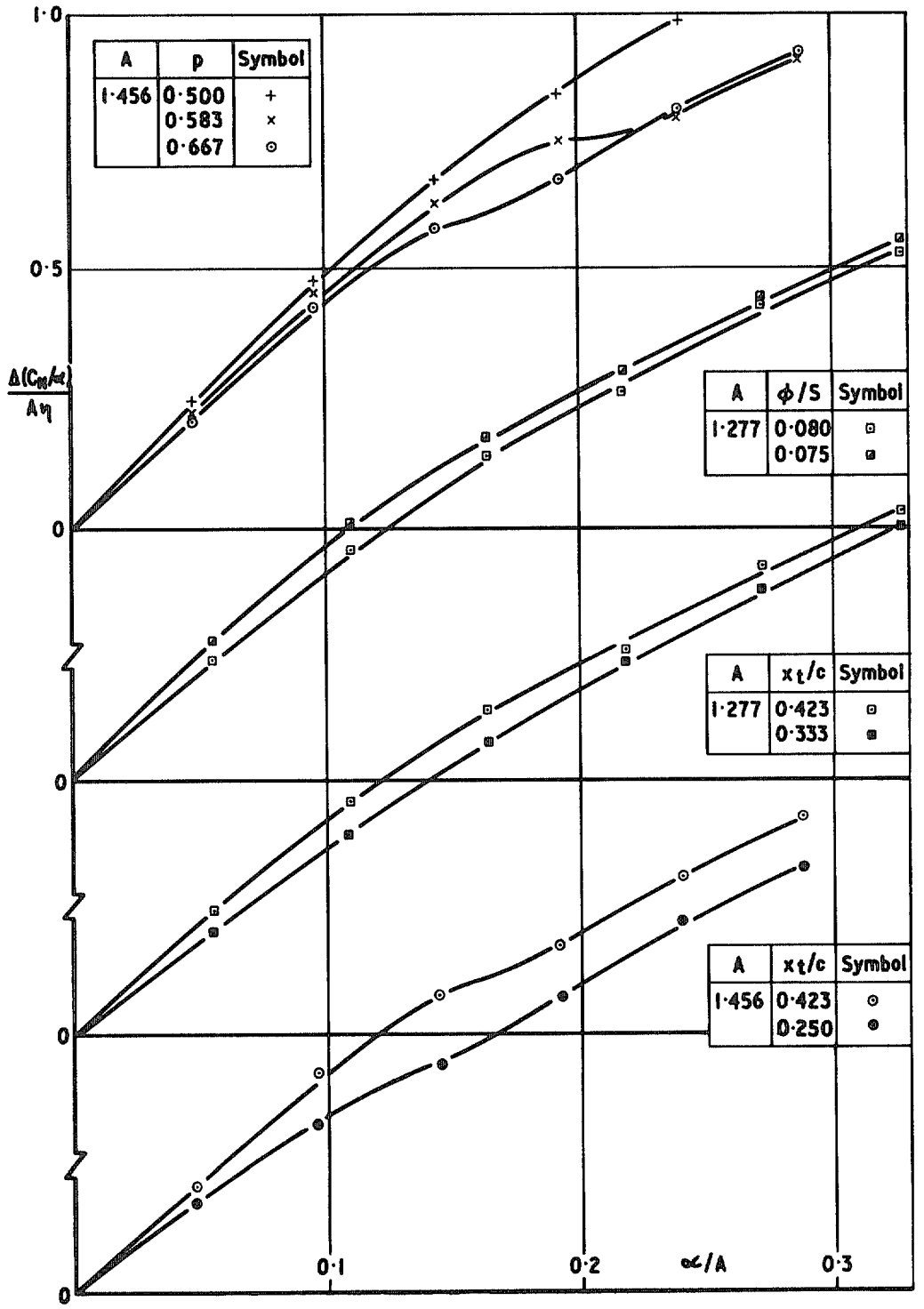

FIG. 11. Variation of $\Delta(C_N/\alpha)/A\eta$ with α/A.

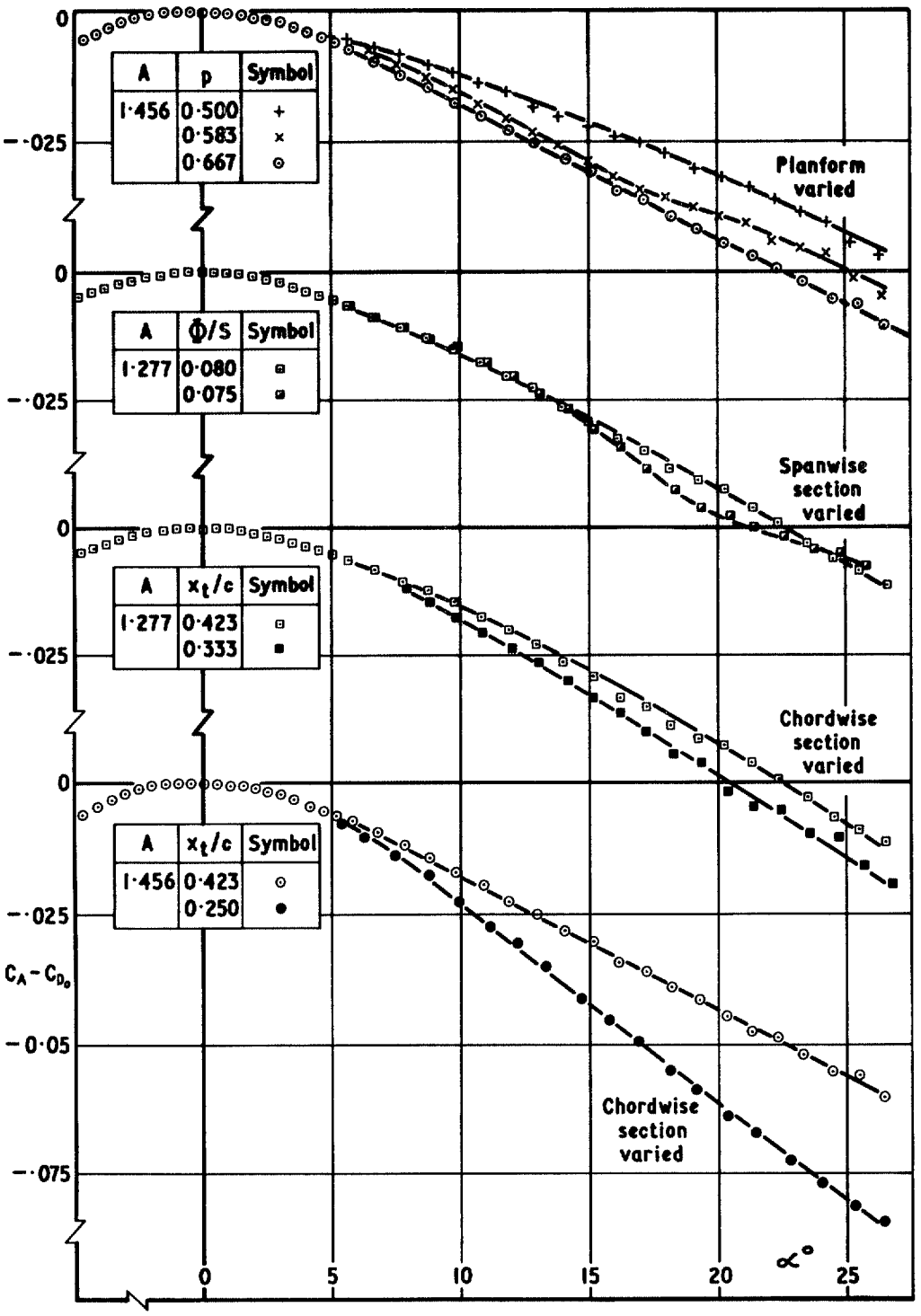

FIG. 12. Variation of $(C_A - C_{D_0})$ with incidence.

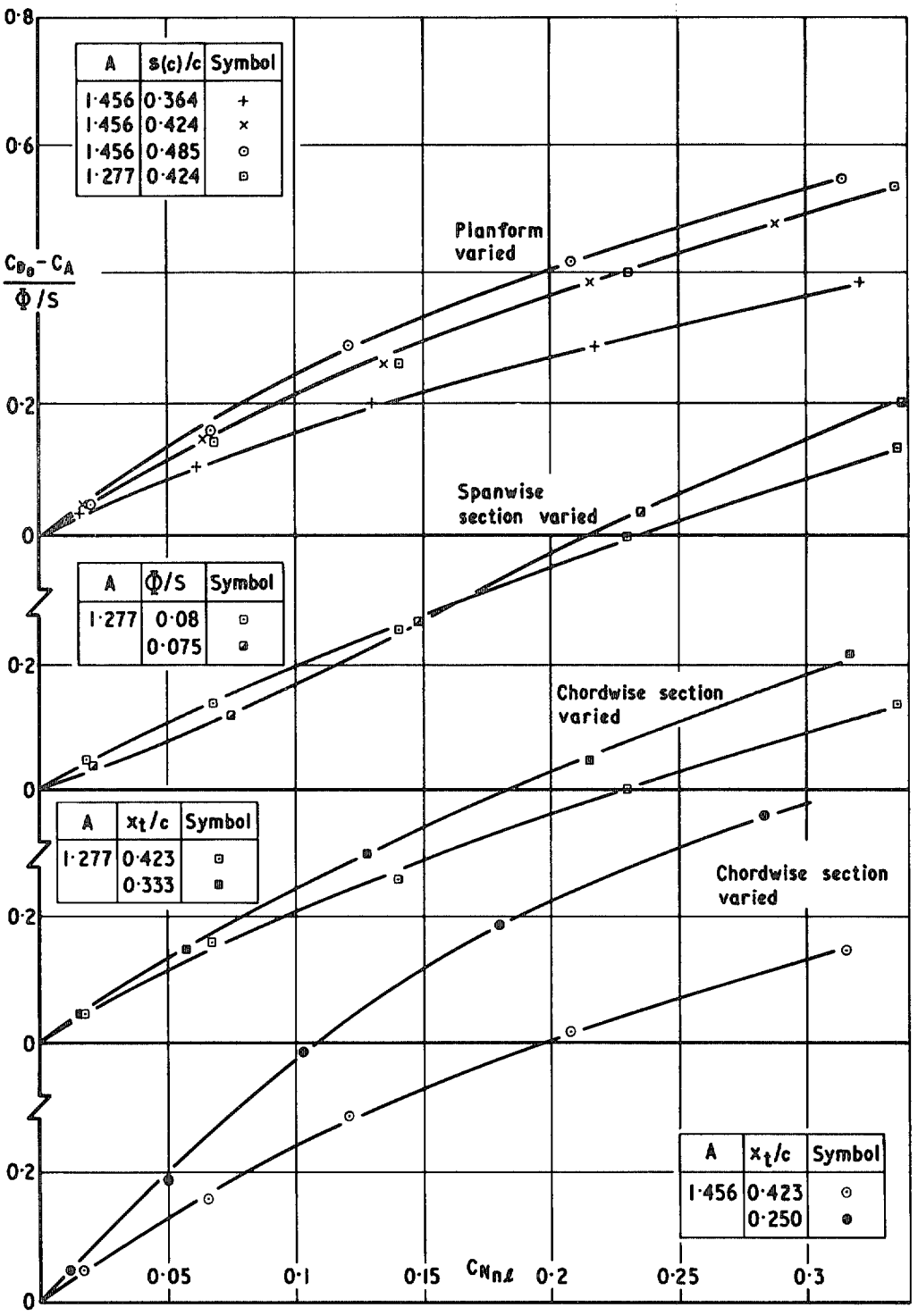

FIG. 13. Variation of $(C_{D_0} - C_A)/\Phi/S$ with $C_{N_{n\ell}}$.

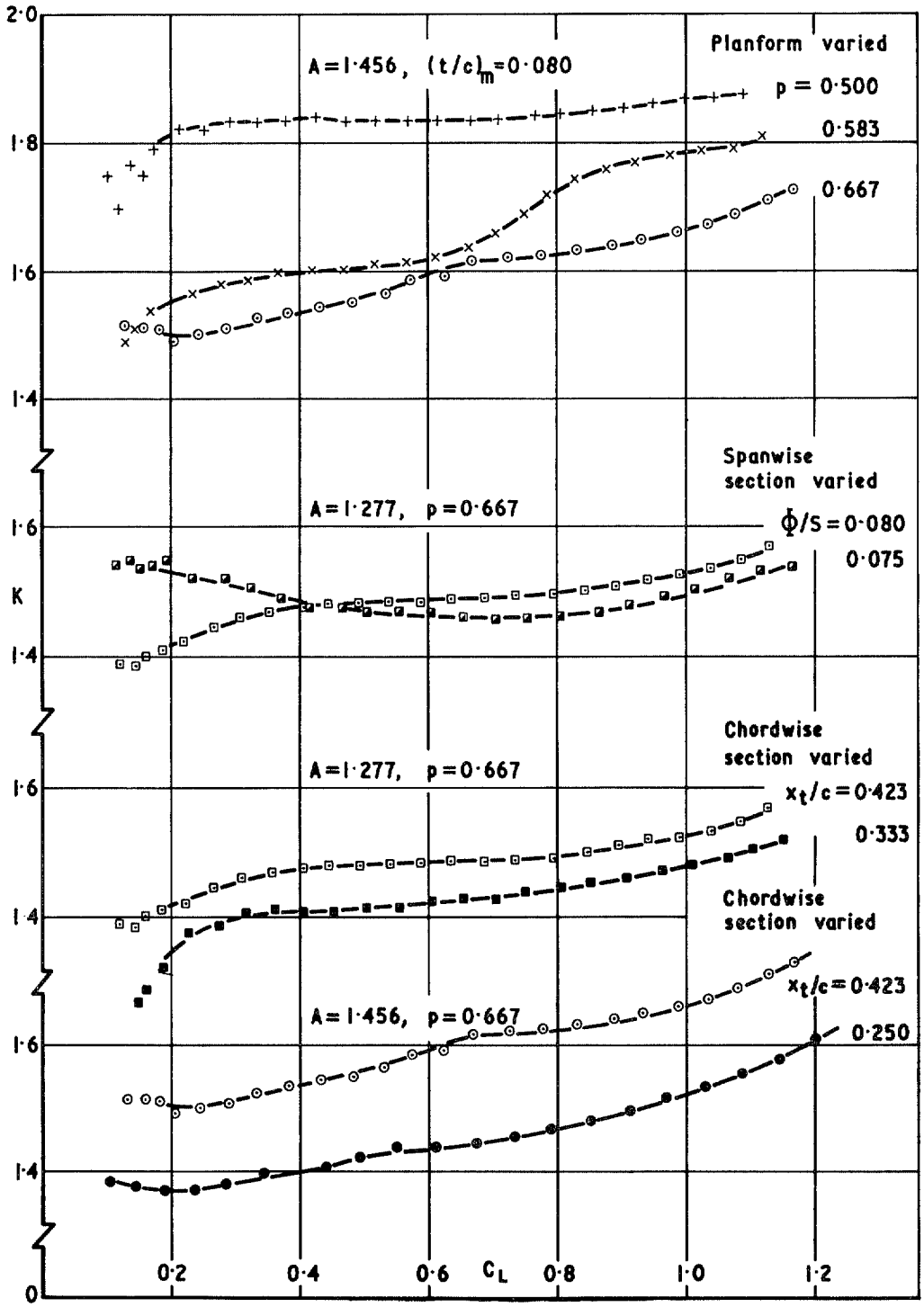

FIG. 14. Variation of K with C_L.

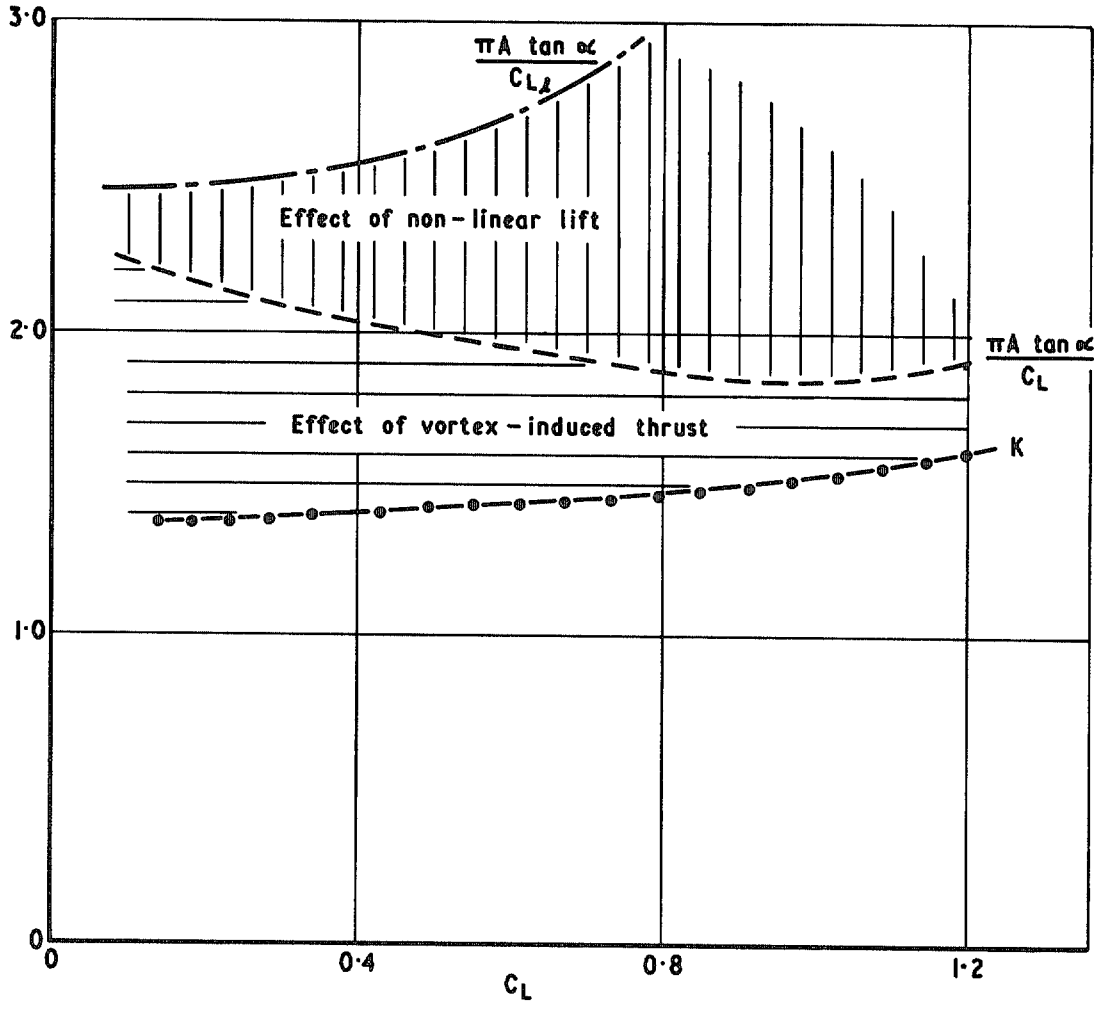

FIG. 15. Comparison of K and $\pi A \tan \alpha / C_L$ for gothic wing ($A = 1{\cdot}456$, $(t/c)_m = 0{\cdot}107$).

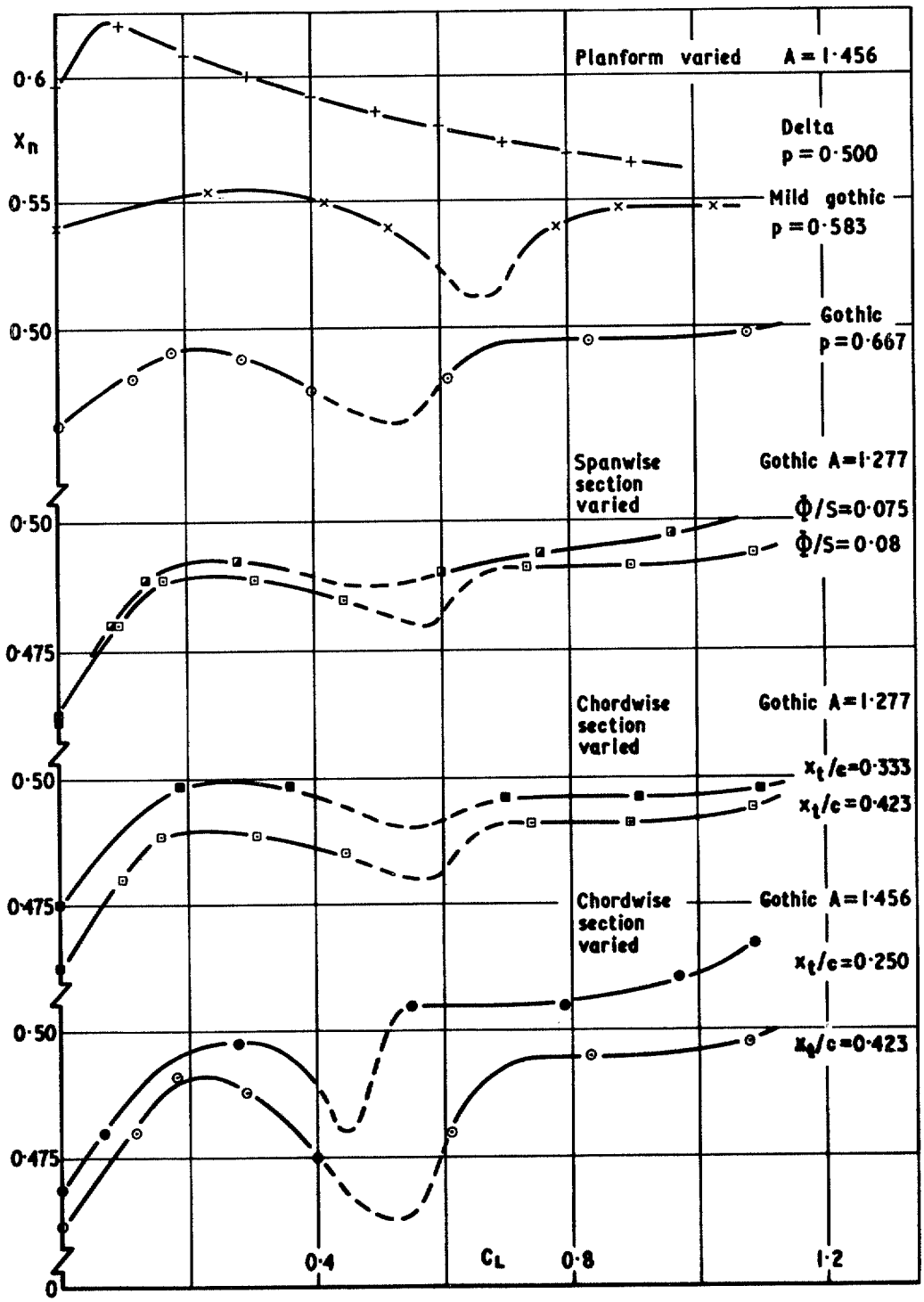

FIG. 16. Aerodynamic centre position.

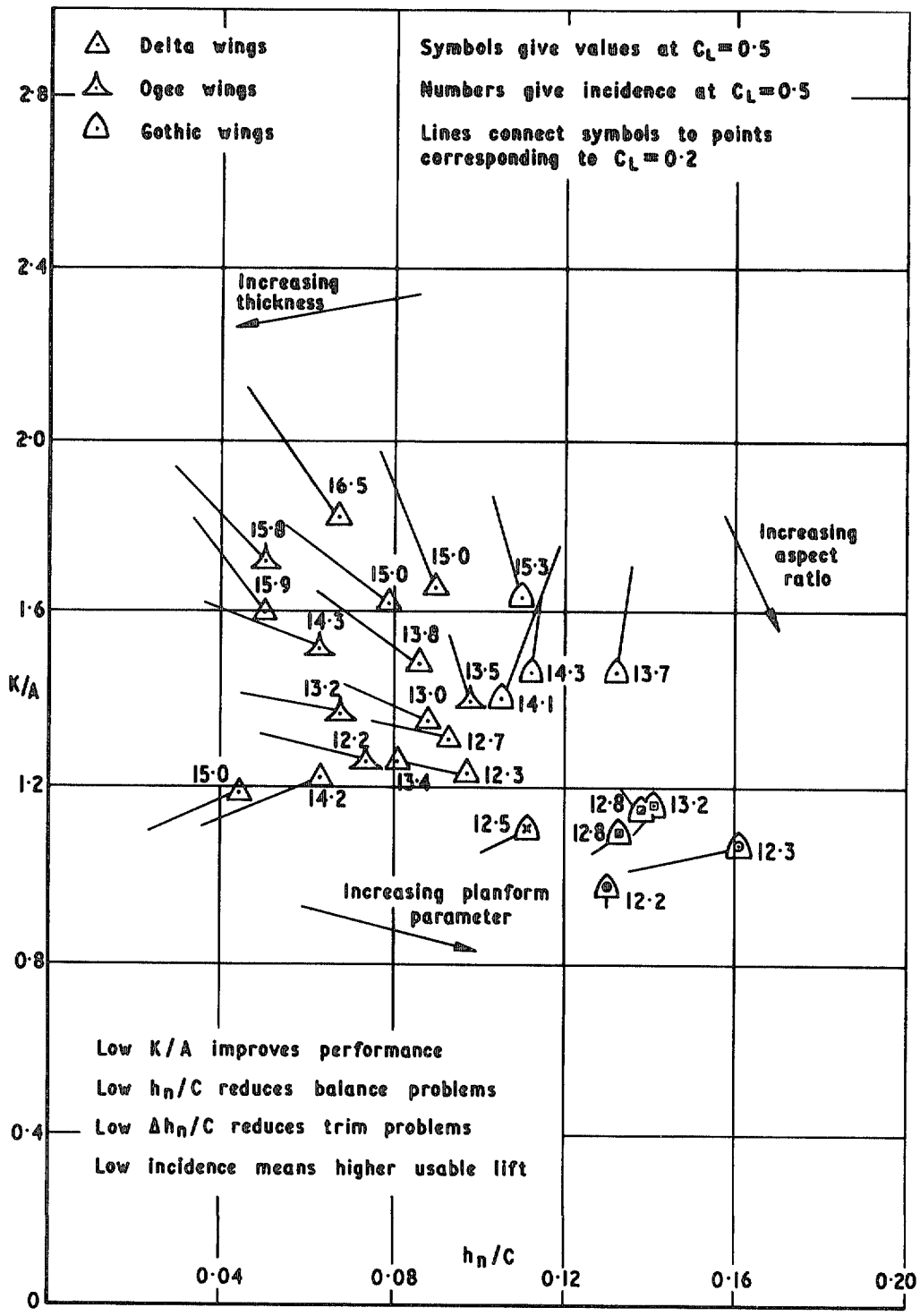

FIG. 17. Lift, drag and stability of slender wings.

Printed in England for Her Majesty's Stationery Office by J. W. Arrowsmith Ltd, Bristol 3
Dd. 503426 K5 4/73

HER MAJESTY'S STATIONERY OFFICE

Government Bookshops

49 High Holborn, London WC1V 6HB
13a Castle Street, Edinburgh EH2 3AR
109 St Mary Street, Cardiff CF1 1JW
Brazennose Street, Manchester M60 8AS
50 Fairfax Street, Bristol BS1 3DE
258 Broad Street, Birmingham B1 2HE
80 Chichester Street, Belfast BT1 4JY

Government publications are also available through booksellers

SBN 11 470520 8